INVESTIGATION ON THE EFFECT OF HUMAN BODY WEIGHT ON BIOMECHANICAL BEHAVIOUR OF FACET JOINTS USING FINITE ELEMENT ANALYSIS

LEE KHAR CHUN

A report submitted
In fulfillment of the requirement for the degree of
Bachelor of Mechanical Engineering (Structure & Materials)

Faculty of Mechanical Engineering

UNIVERSITI TEKNIKAL MALAYSIA MELAKA

2019

DECLARATION

I declare that this project entitled “Investigation on The Effect of Human Body Weight on Biomechanical Behavior of Facet Joints Using Finite Element Analysis” is the result of my own work except as cited in the references.

Signature : ....

Name : ....

Date : ....

APPROVAL

I hereby declare that I have read this project report and in my opinion this report is sufficient in terms of scope and quality for the award of the degree of Bachelor of Mechanical Engineering (Structure & Materials).

Signature	:	………………………………
Supervisor's Name	:	………………………………
Date	:	………………………………

DEDICATION

This project is dedicated to my beloved mother and father for always been there to support and inspire me throughout my life.

ABSTRACT

Obesity is a globally increasing health problem which normally would associate with various kind of diseases such as hypertension, osteoarthritis (OA) and degeneration of soft tissues especially facet joints and intervertebral disc. It is proven that obesity is one of the key contributions that cause low back pain where excessive loading due to obese would change the mechanical behaviour of lumbar spine. The spinal facet joints which serve as one of the load bearers are highly exposed to the risk of joint damage and degeneration when subjected to high mechanical compressive load. Since the concern in studies of facet joints under mechanical compressive load is only given attention in recent years due to difficulties in retrieving its geometrical data and contact pressure. Hence, there is a need to carry out analysis on facet joints especially the effects of human weight on the spinal facet joint. Finite element analysis (FEA) is one of the most suitable method in the study of facet joint since FEA allows repeated simulation which greatly reduce the time consumed and expenditures without compromising the reliability of the results. The main objectives of this study were to improve and verify the FE lumbar spine model and investigate the effects of human weight on the biomechanical behaviour of facet joints through finite element analysis. The ligaments were modelled into the FE lumbar spine model and verified by comparing the intersegmental rotation of the FE lumbar spine model under pure moment of 7.5 Nm in flexion and extension with previous *in vitro* study. The verified FE model was then subjected to compressive follower load of 700 N, 900 N and 1300, which represented the normal weight, overweight and obese weight to investigate the effect of human weight on the kinematics of lumbar spine, stress at capsular ligament and facet contact pressure. The results shown that as compressive load increased, the range of motion for lumbar spine under flexion-extension motion will decrease up to 12%. Besides, it was shown that the stress at capsular ligament and facet contact pressure would increase with increasing compressive load. Under obese weight, the stress at capsular ligament has increased up to 66.75% while facet contact pressure has maximum increment of 19.24% at left superior facets of L3-L4 vertebrae. Therefore, an increase in body weight can change the kinematics lumbar spine and causes an increase in stress at capsular ligament and facet contact pressure. This could be a factor that lead to muscular dystrophy, degeneration of facet joints and osteoarthritis, which are the potential risks for low back pain and chronic low back pain.

ABSTRAK

Obesiti adalah masalah kesihatan yang semakin meningkat secara global dan selalu dikaitkan dengan pelbagai jenis penyakit seperti hipertensi, osteoartritis (OA) dan penyakit cakera degeneratif terutama sendi dan cakera intervertebral. Adalah terbukti bahawa obesiti merupakan salah satu sumbangan utama yang menyebabkan sakit belakang di tulang belakang kerana beban berlebihan akibat obesiti akan mengubah kelakuan mekanikal tulang belakang lumbar. Joint facet spinal yang berfungsi sebagai salah satu penanggung beban sangat terdedah kepada risiko kerusakan sendi dan degenerasi apabila dikenakan beban mampatan mekanikal yang tinggi. Memandangkan keprihatinan dalam kajian mengenai sendi facet di bawah beban mampatan mekanikal hanya diberi perhatian pada tahun-tahun kebelakangan ini disebabkan oleh kesukaran untuk mendapatkan data geometri dan tekanan kontak. Oleh itu, projek ini mengambil kesempatan untuk menjalankan analisis terhadap sendi-sendi facet terutamanya kesan berat badan pada sendi spinal tulang belakang. Analisis unsur terhingga (FEA) adalah salah satu kaedah yang paling sesuai dalam kajian gabungan faset kerana FEA membenarkan simulasi berulang yang dapat mengurangkan masa yang digunakan dan hasil analisis yang tidak menjejaskan kebolehpercayaan keputusan. Objektif utama kajian ini adalah untuk memperbaiki dan mengesahkan model tulang belakang dan mengkaji kesan berat manusia terhadap tingkah laku biomekanik sendi fasa melalui analisis elemen terhingga. Ligamen telah dimodelkan dalam model tulang belakang FE dan disahkan dengan membandingkan putaran intersegmental model tulang belakang FE di bawah momen 7.5 Nm fleksi dan extensi dengan kajian in vitro sebelum ini. Model FE yang telah disahkan kemudiannya dikenakan beban pengikut mampatan 700 N, 900 N dan 1300, yang mewakili berat badan normal, berat badan berlebihan dan obesity untuk menyiasat kesan berat badan manusia pada kinematik tulang belakang lumbar, tekanan pada ligamen kapsul dan aspek tekanan kenalan. Hasilnya menunjukkan bahawa apabila beban mampatan meningkat, pergerakkan tulang belakang lumbar untuk fleksi-extensi akan berkurang sehingga 12%. Selain itu, ia menunjukkan bahawa tekanan pada ligamen kapsul dan tekanan hubungan facet akan meningkat dengan peningkatan beban mampatan. Di bawah berat badan yang obes, tekanan pada ligamen kapsul telah meningkat sehingga 66.75% manakala tekanan hubungan facet mempunyai kenaikan maksimum 19.24% pada bahagian kiri kiri vertebra L3-L4. Oleh itu, peningkatan berat badan dapat mengubah tulang belakang lumbar kinematik dan menyebabkan peningkatan tekanan pada ligamen kapsul dan tekanan hubungan facet. Ini boleh menjadi faktor yang membawa kepada distrofi otot, degenerasi sendi facet dan osteoarthritis, yang merupakan risiko yang berpotensi untuk sakit belakang dan sakit pinggang kronik.

ACKNOWLEDGEMENT

I would like to express my deepest appreciation to my supervisor Dr. Mohd Juzaila Bin Abd Latif for his guidance, advices amd support throughout this project. Secondly, I also want to take this opportunity to show my grattitude towards UTeM, especially Faculty of Mechanical Engineering for the support of facilities and utilities. I would also like to thank my course mates for giving me support and encouragement. Finally, I would like to thank my family for their support and encouragement.

TABLE OF CONTENTS

DECLARATION	
APROVAL	
DEDICATION	
ABSTRACT	i
ABSTRAK	ii
ACKNOWLEDGEMENT	iii
TABLE OF CONTENTS	iv
LIST OF TABLES	vii
LIST OF FIGURES	viii
LIST OF APPENDICES	xi
LIST OF ABBREVIATIONS	xii
LIST OF SYMBOLS	xiv
CHAPTER	
1 **INTRODUCTION**	1
1.1 Background	1
1.2 Problem statement	3
1.3 Objective	4
1.4 Scope	4
2 **LITERATURE REVIEW**	5
2.1 Overview	5
2.2 Biomechanics of human spine	6
2.3 Anatomy of human spine	7
2.4 Human lumbar spine	8
2.4.1 Lumbar vertebra	9
2.4.2 Vertebral body	10
2.4.3 Intervertebral disc	11
2.4.4 Facet joint	12
2.4.5 Ligaments	13
2.5 Low back pain	14
2.5.1 Obesity and low back pain	15

2.5.2 Facet joints related to low back pain 15
2.5.3 Diagnosis 16
2.6 Computational method 16
2.6.1 Finite element model of spine 17
2.6.2 Finite element modelling of ligaments 18
2.6.3 Material properties of human lumbar spine 18
2.6.4 Follower load method 24
2.6.5 Finite element studies of mechanical behavior of human lumbar spine 25
2.6.6 Range of motion 26
2.6.7 Intradiscal pressure of intervertebral disc 26
2.6.8 Stress analysis of facet joint 26
2.7 Research gap of knowledge 27

3 **METHODOLOGY** 28
3.1 Overview 28
3.2 Development of 3-D model of lumbar spine 29
3.3 Finite element model of lumbar spine 31
3.4 Material properties 32
3.5 Development of ligaments 33
3.6 Loading and boundary condition 36
3.7 Verification of finite element model 38
3.7.1 Intersegmental rotations of the lumbar spine 38
3.7.2 Intervertebral disc 38
3.8 Finite element analysis of the lumbar spine model under different groups of human weight 39

4 **RESULTS AND DISCUSSION** 40
4.1 Overview 40
4.2 The effects of ligaments in lumbar spine model 40
4.2.1 Intersegmental rotation of lumbar spine model 40
4.2.2 Intersegmental rotation of lumbar spine model with ligaments 42
4.2.3 Intervertebral disc (IVD) 43
4.3 Verification of human lumbar spine model with hyperelastic ligaments 44

4.3.1 Intersegmental rotation of lumbar spine model with hyperelastic ligaments 44
4.3.2 Verification of intervertebral disc 45
4.4 Biomechanical effects of human weight on FE lumbar spine model 46
4.4.1 The effects of human weight the kinematics of lumbar spine 46
4.4.2 The effects of human weight on the stress at capsular ligament 49
4.4.3 The effects of human weight on facet contact pressure 50

5 **CONCLUSION AND RECOMMENDATION FOR FUTURE RESEARCH** 60
5.1 Conclusion 60
5.2 Recommendations for future research 61

REFERENCES 62
APPENDIX A 74
APPENDIX B 78

LIST OF TABLES

TABLE	TITLE	PAGE
2.1	The material properties used to model lumbar spine in previous studies.	21
3.1	Material properties used in the FE lumbar spine model 1.	32
3.2	Material properties used in the FE lumbar spine model 2	32
3.3	Material properties used in the FE lumbar spine model 3.	33
3.4	Geometrical parameters of the lumbar spine ligaments	34
3.5	Type 1 (elastic) material properties used for ligaments	34
3.6	Type 2 (nonlinear) material properties used for ligaments	35
3.7	Magnitude of moment loading applied on lumbar spine model	37

LIST OF FIGURES

FIGURE	TITLE	PAGE
1.1	The disc and facet joints of the spine. (A) Posterior view. (B) Right lateral view of sagittal plane cross section. (Muscolino, 2014).	2
2.1	Anatomic reference directions (Kurtz and Edidin, 2006)	5
2.2	Types of motions of the spine. (Kurtz and Edidin, 2006)	6
2.3	Microscopic Anatomy of Spine (Sarathi Banerjee, 2013)	7
2.4	Left lateral view of the lumbar spine. (Netter, 2014)	8
2.5	Superior view of L2 vertebra. (Netter, 2014)	9
2.6	The structure of normal vertebra bone. (Netter, 2014)	10
2.7	A cut out portion of normal intervertebral disc (Raj, 2008)	11
2.8	The IVD under (a) Compressive loading and (b) Bending. (White and Panjabi, 1990)	12
2.9	The lumbar L3-L4 facet joints. (Bogduk, 2005)	13
2.10	Ligaments attached to lumbar spine. (Netter, 2014)	14
2.11	Two types of spine models a. Whole-spine model (Lee et al., 1995) b. Vertebral-segment model (Teo et al., 2004)	17
2.12	Models of ligament in truss element on FE lumbar spine (Fan and Guo, 2018).	18
2.13	A typical stress-strain curve for biological tissue. AB, the neutral zone; BC, the elastic zone. When the elastic limit (yield point C) is reached, permanent deformation can occur (permanent set). CD, the plastic zone where permanent set occurs. Past D, failure occurs, and the load diminishes. (Samandouras, 2010)	20

2.14	The application of (a) Compressive vertical load (b) Compressive follower load (Patwardhan et al., 1999)	24
2.15	Orientation of facet joints (Hall, 1991)	25
3.1	Methodology flow chart	29
3.2	CT scan data of human spine	30
3.3	STL 3-D model of L1-L5 lumbar vertebrae.	30
3.4	3-D FE model of the lumbar spine	31
3.5	FE modelling of the ligaments attached at the lumbar spine (a) posterior (b) lateral views	34
3.6	Loading and boundary condition on FE lumbar spine model	37
4.1	The comparison of total ROM of the lumbar spine between FE models and previously published in vitro result (Panjabi et al., 1994) under pure moment from -7.5 Nm to 7.5Nm.	41
4.2	Deformation of lumbar spine model under flexion and extension rotation	42
4.3	The comparison of total ROM of the lumbar spine between FE models (with elastic ligaments and without ligaments) and previously published in vitro result (Panjabi et al., 1994) under pure moment from -7.5Nm to 7.5Nm.	43
4.4	Comparison of present FE Model (with and without elastic ligaments) and previous *in vitro* studies of the IVD results (a) axial displacement (b) intradiscal pressure under compressive load up to 1200N	44
4.5	The comparison of total ROM of the lumbar spine between FE models (with hyperelastic ligaments) and previously published in vitro result (Panjabi et al., 1994) under pure moment from -7.5Nm to 7.5Nm.	45
4.6	Comparison of present FE Model (hyperelastic ligaments) and previous *in vitro* studies of the IVD results (a) axial displacement (b) intradiscal pressure under compressive load up to 1200N.	46

4.7	Intersegmental rotation for normal, overweight and obese under flexion and extension motion.	47
4.8	Intersegmental rotation for flexion-extension under normal, overweight and obese load.	48
4.9	Stress at capsular ligament	49
4.10	Left and right superior facet contact pressure under flexion motion.	50
4.11	Left and right inferior facet contact pressure under flexion motion.	51
4.12	Left and right superior facet contact pressure under extension motion	51
4.13	Left and right inferior facet contact pressure under extension motion	52
4.14	Pressure distribution for flexion under normal weight	54
4.15	Pressure distribution for flexion under obese weight	55
4.16	Pressure distribution for extension under normal weight	57
4.17	Pressure distribution for extension under obese weight	58

LIST OF APPENDICES

APPENDIX	TITLE	PAGE
A1	L1 anterior vertebrae dimension details	
A2	Disc Specification (Length and Width)	
A3	Disc Specification (Thickness)	
A4	Superior and Inferior Facet Joint Specification	
B	Case study – simulation data results	

LIST OF ABBREVIATION

FEM	Finite element method
LBP	Low back pain
DDD	Disc degeneration disease
IVD	Intervertebral disc
AF	Annulus fibrosus
NP	Nucleus pulposus
L1	The first lumbar vertebra
L2	The second lumbar vertebra
L3	The third lumbar vertebra
L4	The fourth lumbar vertebra
L5	The fifth lumbar vertebra
FEA	Finite element analysis
TDR	Total disc displacement
FE	Finite element
ROM	Range of motion
IDP	Intradiscal pressure
PLL	Posterior longitudinal ligament
ALL	Anterior longitudinal ligament
LF	Ligamentum flavum
CL	Capsular ligament

ITL	Intertransverse ligament
ISL	Interspinous ligament
SSL	Supraspinous ligament
OA	Osteoarthritis

LIST OF SYMBOLS

E	-	Young's modulus
v	-	Poisson's ratio
C_1, C_2	-	Material constant characterizing the deviatoric deformation
M	-	Moment
F	-	Force
D	-	Displacement

CHAPTER 1

INTRODUCTION

1.1 Background

Low back pain (LBP) is a health disorder that happens in all especially developed countries and at all age groups. It is reported that about 84% from populations would suffer low back pain in their lifetime (Balagué et al., 2012). LBP is a pain or muscle tension that happens at the lumbar region and could lead to disability and work absenteeism which cause increasing health care cost and socioeconomic burden (Manusov, 2012, Koes et al., 2006).

The causes of LBP include degeneration of intervertebral discs as well as osteoarthritis of facet joints (Schwarzer et al., 1994, Weishaupt et al., 1998). Facet joint is a synovial joint in human spine which locate between the articular processes of two adjacent vertebrae as shown in Figure 1.1. The facet joints play a vital role in transmission of load and stabilise the motion of spine such as flexion and rotation. They also restrict the range of motion for axial rotation. On statistics, study shows that about 15% to 40% of low back pain is due to the facet joint (Dreyer and Dreyfuss, 1996). Osteoarthritis can be defined as degeneration of lumbar facet joints where cartilage cushion deteriorates that lead to formation of osteophyte and subchondral bone sclerosis (Kalichman and Hunter, 2007). This results in the joint pain and reduced flexibility due to rubbing of two adjacent vertebrae.

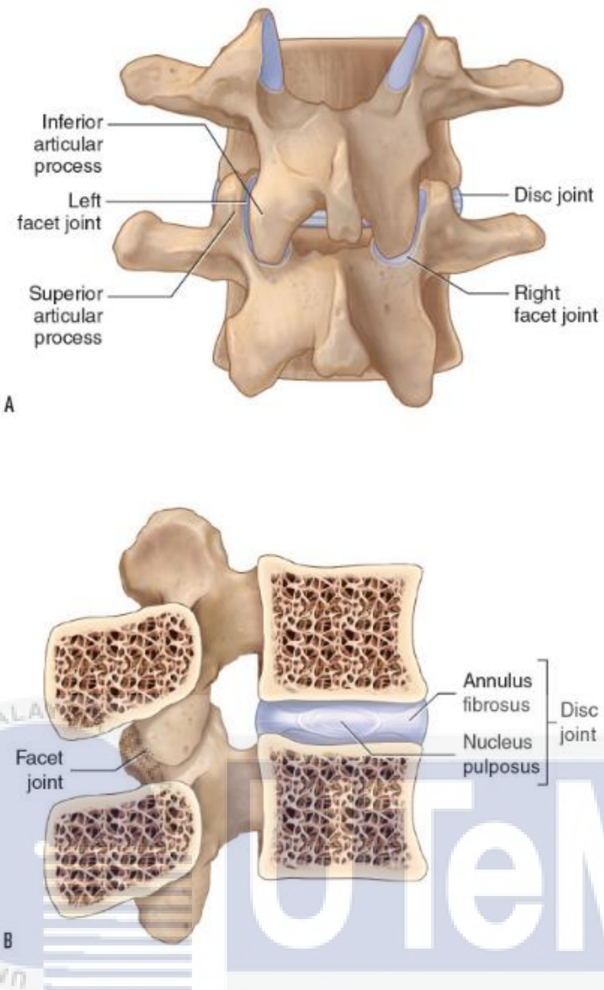

Figure 1.1: The disc and facet joints of the spine. (A) Posterior view. (B) Right lateral view (Muscolino, 2014).

Factors that could lead to LBP include aging, excess weight, smoking habit, poor posture or genetics inherence. All these factors especially obesity could lead to osteoarthritis (OA) at the lumbar facet joint which is reported as possible cause low back pain (Gellhorn et al., 2013, Manchikanti et al., 2016, Walker, 2000). In anatomical perspective, the increased weight will burden the mechanical loading on the lumbar spine, which could cause changes of structure such as osteoarthritis (Peng et al., 2018). Obesity has also been recognised as pandemic. Statistics showed that there has been increased of 28% in adult on prevalence of overweight between 1980 and 2013 (Smith and Smith, 2016).

In order to clearly rectify the relationship between degenerative facet joints from obesity and biomechanical effect of lumbar spine, finite element analysis (FEA) is a good approach to study the relationships. The model of lumbar spine is simulated using FEA which is a computational technique that discretizes the model into finite elements and demonstrates the behaviour of the elements. The FEA is a decent method to be implemented as it provides precise and fast simulation results while allowing repetition of simulation, quick calculation time and cost saving.

1.2 Problem Statement

Previous studies verified that obesity brings significant effect on low back pain (LBP) and with the increasing of prevalence for obesity, this case is predicted to hike in the future (Leboeuf-Yde, 2000, Shiri et al., 2008, Shiri et al., 2010). Obesity also results in increased mechanical stress and would affect the mechanical behaviour at the joint (Leboeuf-Yde, 2000, Vincent et al., 2012).

While FEA studies on biomechanical behaviour of lumbar vertebrae has been widely carry out by previous studies, some of the studies did not implement the whole lumbar vertebrae in the FE models (Schmidt et al., 2008, Goel et al., 1993, Zahari et al., 2017). Besides, modelling of capsules is sometimes given less emphasis and instead contact pair surface method is used to represent capsular ligaments of facet joint (Kuo et al., 2010).

Therefore, this study aimed to examine the effect of human body weight on the facet joint using an improved lumbar spine model.

1.3 Objective

There are two main objectives in this study:

1) To improve and verify the finite element model of the lumbar spine.
2) To investigate the effect of human body weight on the biomechanical behaviour of facet joints.

1.4 Scope

In this study, capsular ligaments in the facet joints of lumbar spine were modelled in existing FE lumbar spine model using ABAQUS software to replicate the actual physiological behaviour of the spine. Then, the lumbar spine model was verified with the previous experiment study to make sure simulation results are valid. The stresses at the facet joints were examined at different human weight and different spine motion such as flexion and extension.

CHAPTER 2

LITERATURE REVIEW

2.1 Overview

This chapter discusses about LBP and human lumbar vertebrae. The FEA of lumbar vertebrae will also be outlined as it brings remarkable results for future research to reduce problems on real human lumbar vertebrae. Throughout this study, the anatomy directions of human body are shown according to the terms in Figure 2.1.

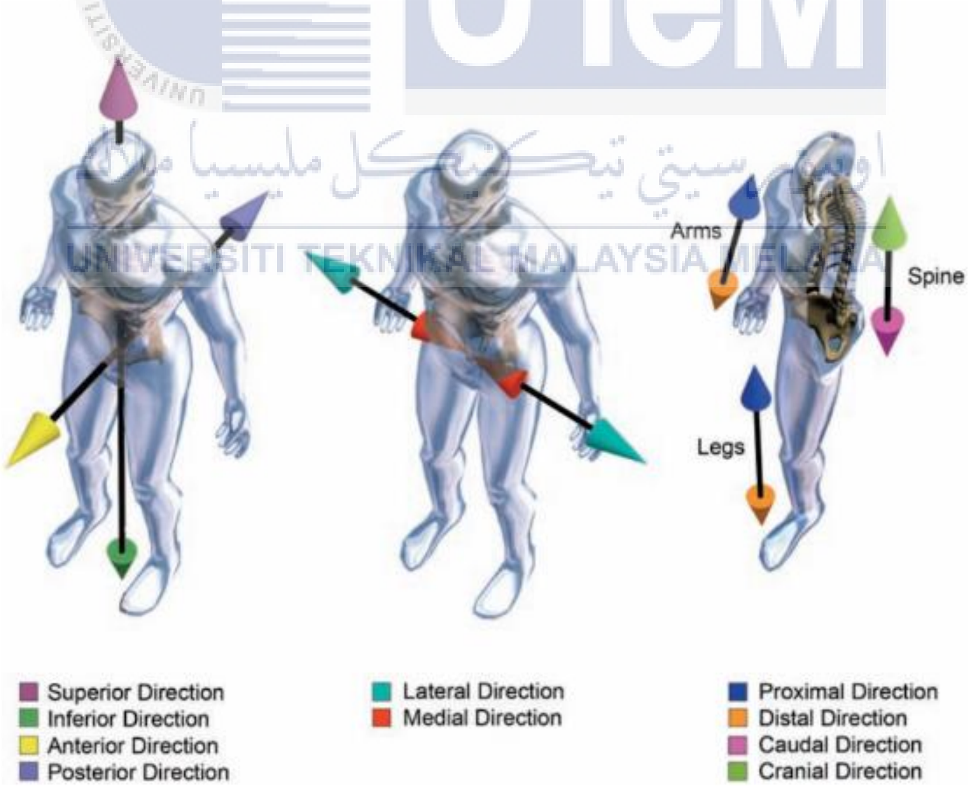

Figure 2.1: Anatomic reference directions (Kurtz and Edidin, 2006).

2.2 Biomechanics of human spine

Biomechanics of spine shows the study of structure and function of spine in mechanical aspects. It is important as it help us to understand how our body structures work and function especially our skeletal system. In order to gain more understanding on human spine which acts as main support for human body and stability, the application of biomechanics study of human spine is important and need to be carried out from time to time.

The biomechanical intents of spine are to serve as structural support for the body while permitting trunk movement as shown in Figure 2.2. It also protects the nerves that connect periphery to brain. The integration of spine stability and mobility is important to achieve these roles concurrently (Bergmark, 2009). The spine also distributes the upper body weight to pelvis with internal forces outnumber the whole-body weight. The kinematics motion patterns of spine are complex due to its flexibility. However, it can be classified into flexion, extension, lateral bending, and axial rotation. (Sarathi Banerjee, 2013)

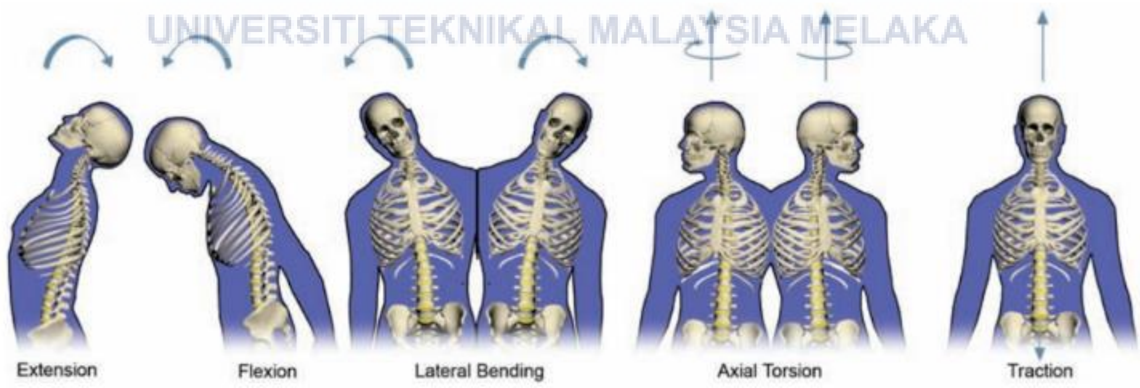

Figure 2.2: Types of motions of the spine. (Kurtz and Edidin, 2006)

2.3 Anatomy of human Spine

The structure of human spine must be rigid enough to support the body weight and strong to protect spinal cord. It also needs to be flexible to allow movement in various directions (Devereaux, 2007). The spine is form by assembly of many discrete bony elements called vertebrae that held by restraints of ligaments. Intervertebral disks are found between the vertebrae. Each of them forms an articulating joint with two vertebrae which known as Functional Spine Units (FSU).

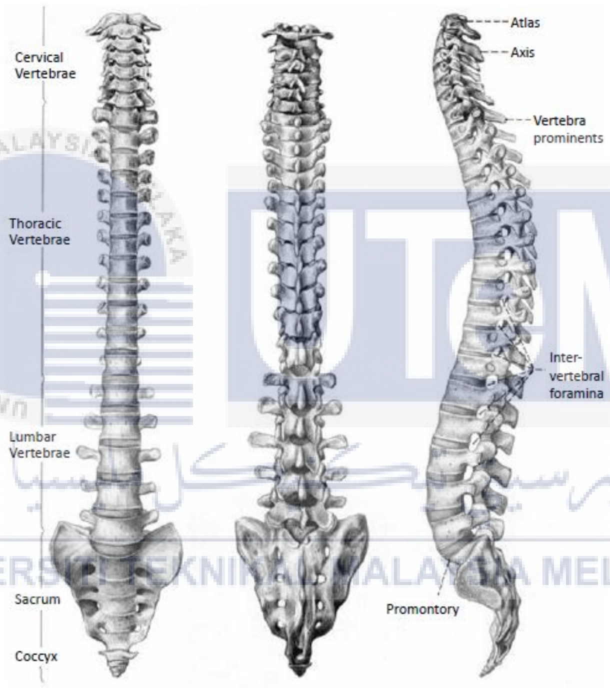

Figure 2.3: Microscopic Anatomy of Spine (Sarathi Banerjee, 2013).

Human spine is comprised of cervical, thoracic, lumbar, sacrum and coccyx regions as illustrated in Figure 2.3 (Sarathi Banerjee, 2013). The cervical spine consists of 7 vertebrae that locate at the neck region. Cervical vertebrae are the first 7 vertebrae in the human spine that provide flexibility for motion of head. Thoracic spine made up of 12 thoracic vertebrae that locate just after cervical spine. The lumbar spine consists of 5 lumbar vertebrae which bear highest loads and moments of spine. The sacrum is an assembly of 5 vertebrae that attach to L5 with pelvis. The coccyx is located at the terminal of spine and often called as tail bone (Kurtz and Edidin, 2006).

2.4 Human Lumbar Spine

The lumbar spine is located below the cervical spine and thoracic spine. Normally, people have five bones (vertebrae) in the lumbar spine as displayed in Figure 2.4. Human lumbar spine is vital in supporting the upper body weight and any external loads without deformation. It also maintains perfect flexibility and stability of the body to carry out daily activities (Han et al., 2011).

An IVD connects two vertebrae and articulating facet joints as shown in Figure 2.4. This pattern repeats to the end of the inferior part of lumbosacral junction L5, where the vertebrae is connected to sacrum via intervertebral disc and articulating facet joints (Netter, 2014).

Figure 2.4: Left lateral view of the lumbar spine. (Netter, 2014)

2.4.1 Lumbar vertebra

The lumbar vertebrae are the largest and heaviest vertebrae in spine. They are located at lumbar region which is below cervical and thoracic regions. As illustrated in Figure 2.5, it has a kidney shape when view superiorly, which is wider from the side to side than front to back (Ebraheim et al., 2004). Each lumbar vertebra can be divided into two parts, which are anterior part and posterior part. The anterior part consists vertebral body while vertebral arch is located at posterior part which consists of two laminae, two pedicles and seven processes that together surround the vertebral foramen. The seven processes are the spinous process, two transverse processes, two superior facets and two interior facets.

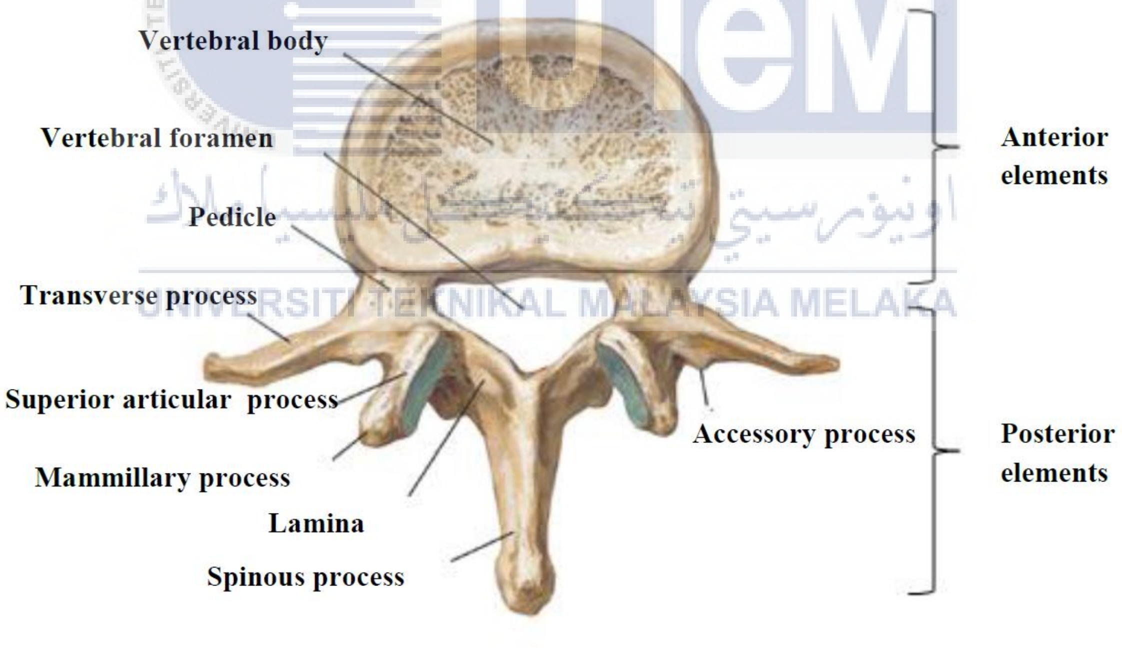

Figure 2.5: Superior view of L2 vertebra. (Netter, 2014)

2.4.2 Vertebral body

The vertebral body consists cortical shell which encloses the cancellous bone as shown in Figure 2.6. The cortical bone, which also known as compact bone is a high-density bone that forms a protective cavity. It is vital in weight bearing due to its superb resistance towards bending and torsion. Moreover, the cancellous bone, which also known as spongy bone is a light and porous bone that consists a network of large spaces that give a spongy and honeycombed appearance.

In fact, the cancellous bone is weaker than cortical bone because of its less density. However, cancellous bone provides greater flexibility which enables it to dampen sudden stresses. It also able to resist greater changes in unit shape when loads are applied to it (White and Panjabi, 1990).

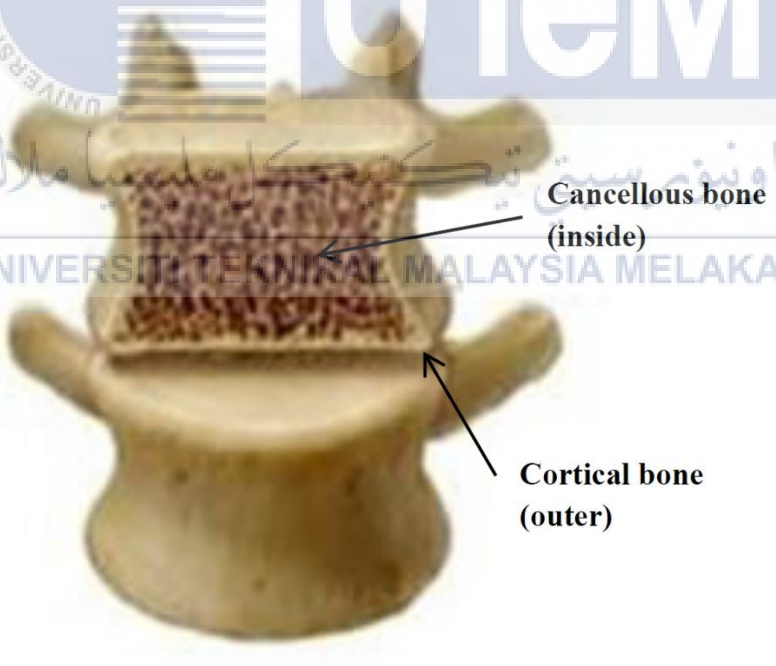

Figure 2.6: The structure of normal vertebra bone. (Netter, 2014)

2.4.3 Intervertebral disc

The intervertebral disc (IVD) is situated between two adjacent vertebral bodies. It is a fibrocartilaginous cushion which is important in absorbing shock in spine. IVD are the primary joints of the spinal column and is responsible for one third of its height. As illustrated in Figure 2.7, the intervertebral discs consist a thick outer ring of fibrous cartilage known as annulus fibrosus, which encloses the nucleus pulposus, a more gelatinous core. (Raj, 2008).

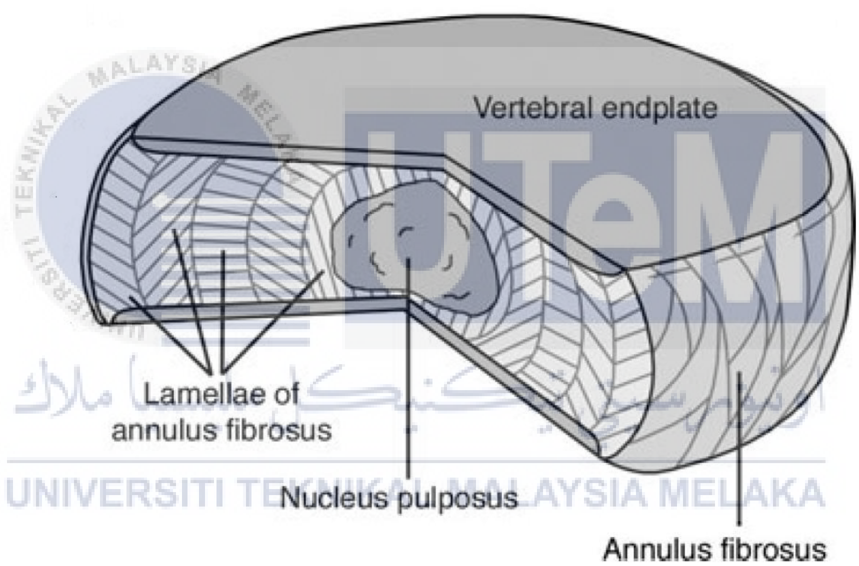

Figure 2.7: A cut out portion of normal intervertebral disc (Raj, 2008).

The annulus is made up of 15 to 25 layers of concentric rings, which also known as lamellae, with each lamella having collagen fibres lying parallelly (Urban and Roberts, 2003). The fibres are approximately 60° oriented to the vertical axis, alternate to the left and right in adjacent lamellae. The annular fibres play vital role in preventing nucleus pulposus from herniating.

Nucleus pulposus contains collagen fibres that are organized irregularly, and elastin fibers which arranged radially. These fibers are embedded in a highly hydrated aggrecan-containing gel (Raj, 2008). The nucleus pulposus together with entire IVD support in shock absorption for the spine by reallocating the forces and cushion sudden loads as shown in Figure 2.8.

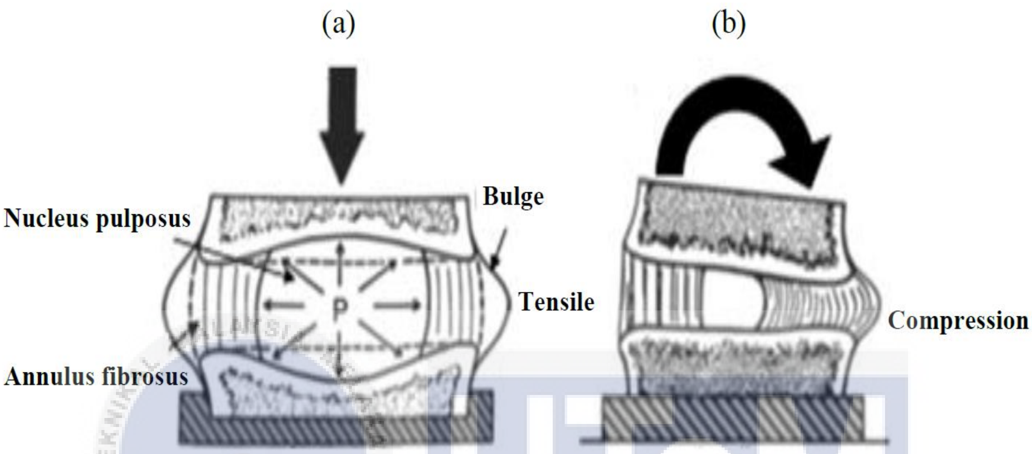

Figure 2.8: The IVD under (a) Compressive loading and (b) Bending. (White and Panjabi, 1990)

2.4.4 Facet joint

The spinal facet joint is also known as zygapophyseal joint. It is situated at the posterior side of spine and connects to inferior and superior processes of adjacent vertebrae as shown in Figure 2.9. In each vertebrae, there are one set of superior articular facets and one set of inferior articular facets (Bogduk, 2005).

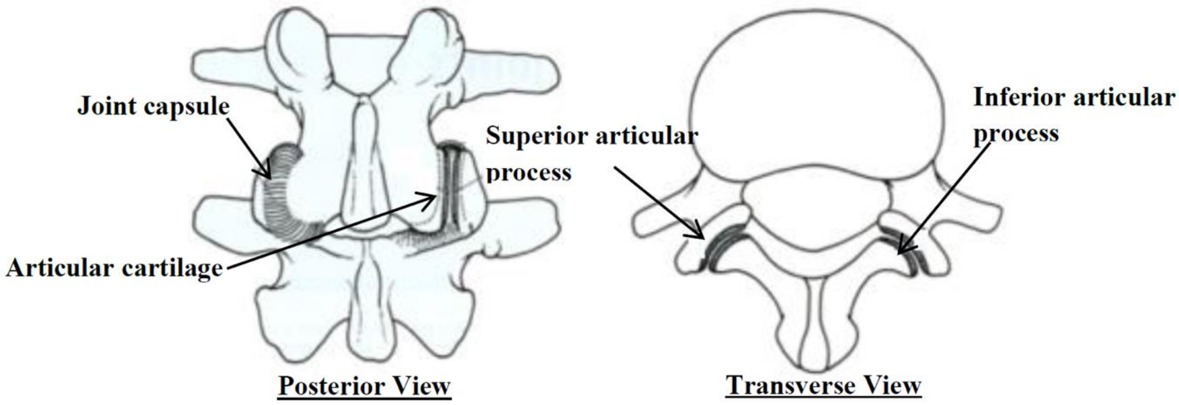

Figure 2.9: The lumbar L3-L4 facet joints. (Bogduk, 2005)

Facet joint is recognised as synovial joint: the two facing surface of facets are coated by articular cartilage and covered with ligamentous capsules. The joints are nourished and lubricated by the synovial fluid which produced from the connective tissue of the capsule. The facet joints are important in maintaining mechanical stability of the spine. The relative motions of two adjacent vertebrae that could overload and damage the spine structure such as intervertebral disc and nerve root are prevented by facet joints (Jaumard et al., 2011b). Besides, facet joints also help in load transmission. In normal facet joint, about 3 to 25% of segmental load are transmitted over it (Kalichman and Hunter, 2007).

2.4.5 Ligaments

Ligaments are dense, white, hypovascular bands of collagenous fibers that form joints at both ends of bone (Bray et al., 2005). The functions of ligaments include they act as primary passive stabilizers of joints through an optimum range of motion for joints and protect other articular tissues from aberrant force (Miller and Thompson, 2003).

In general, there are seven spine ligaments which are anterior and posterior longitudinal ligaments (ALL & PLL), inter and supraspinous ligaments (ISL & SSL), ligamentum flavum (LF), facet capsular ligaments (CL) and intertransverse ligaments (ITL) as illustrated in Figure 2.10.

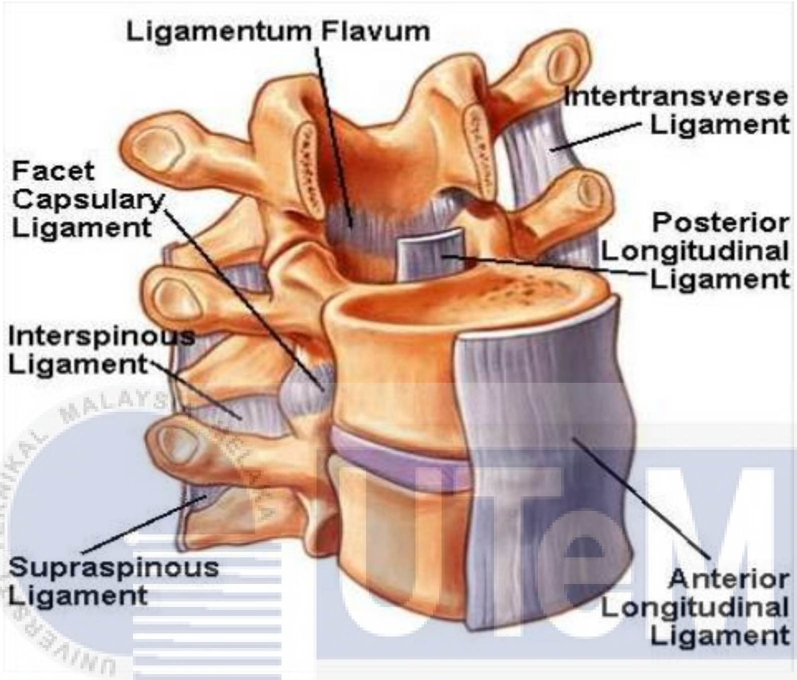

Figure 2.10: Ligaments attached to lumbar spine. (Netter, 2014)

2.5 Low back pain

Low back pain is a pandemic health problem that happens globally and especially in all developed countries (Koes et al., 2006). Statistically, approximate 74% from populations would suffer low back pain throughout their lifetime and there is 54% of increment of populations that suffer low back pain between 1990 and 2015 (Hartvigsen et al., 2018, Balagué et al., 2012). Low back pain is clearly a pain suffer at lower back at the lumbar region. Most people with low back pain will also suffer pain in one or both legs while some have neurological symptoms at lower limbs. There are lots of causes that lead to LBP and some of the most common causes are obesity and degeneration of facet joint (Hartvigsen et al., 2018, Deyo, 1992).

2.5.1 Obesity and low back pain

Obesity is a growing health issue in developed countries which lead to various illness such as musculoskeletal disorders, including osteoarthritis and low back pain (Vismara et al., 2010). Human weight are normally categorised into underweight (BMI of <18.5kg/m^2), normal weight (BMI of 18.5kg/m^2 to 25.0kg/m^2), overweight (BMI of >25kg/m^2) and obese (BMI of >30kg/m^2) (Flegal et al., 2013). The Body Mass Index (BMI) is a mathematical formula (BMI=weight in kg/square of height in m^2) that use to indicate a person's state of weight. The higher BMI value of a person above 25kg/m^2, the higher the tendency of that person to become obese, and higher potential to suffer from health disorders (NIDDK, 2001).

According to Vismara et al. (2010), the prevalence of osteoarthritis among obese population is about 34%, which include 17% at knee, 7% at spine level and 10% at other joints. Since LBP is correlated linearly with BMI where prevalence of LBP increased in the obese populations, it is important to examine the effect of human weight on the biomechanical behaviour of spine to reduce musculoskeletal pain (Leboeuf-Yde, 2000).

2.5.2 Facet joint related to low back pain

In normal condition, the facet joints fit together clingy and glide smoothly without any pressure generated. However, if there is pressure built at the joint, the cartilage on the joint will wears off or erodes and this phenomenon is called as degeneration of facet joints. The degenerated cartilage could cause abnormal motion or even hypermobility of the facet joint (Fujiwara et al., 2000). In some cases, osteophyte formation might also occur which is the most conspicuous remodelling phenomena in facet joint osteoarthritis. The joints that shoe osteophyte formation is believed to have more severe degeneration then those without osteophyte (Gellhorn et al., 2013).

2.5.3 Diagnosis

There are several ways to do diagnosis on low back pain. The simplest diagnostic methods are complete medical history and physical examination. For severe case, imaging test will be carried out for diagnosis. There are two types of imaging test which are magnetic resonance imaging (MRI) and computed tomography (CT) scan. The CT scan can show problems in the bone tissue and near the facet joints such as bone spurs. On the other hand, MRI gives a clear picture of the soft tissues of the body.

2.6 Computational method

A finite element method (FEM) is a numerical technique used to obtain an approximate solution to a complex problem by differential equations and aims to help us to comprehensively understand and quantify any physical phenomena. Nowadays, the computational techniques have also been applied in the study of cell, tissue and organ biomechanics. The finite element method has become an effective alternative for in vivo surgical assessment since decades. The use of computational method on lumbar spine can help to solve many problems without being subjected to limitations that related to the behaviour of the body alive. (Anderson et al., 2007). However, the model generated through computational method for a specific purpose should be validated with respect to that purpose.

A computerized model also needs to be verified to ensure that the implementation of method is correct (Anderson et al., 2007).

2.6.1 Finite element model of spine

The human spine models can be categorised into 2 types which are the whole-spine models and the vertebral-segment models, as illustrated in Figure 2.11. Generally, the whole-spine models comprised of simplified components of the spine that use to study the structural behaviour of the whole spine column. These models are used to estimate the biomechanics behaviour of different elements in spine. However, the models are unable to determine reliable results for soft tissue and vertebrae. Therefore, vertebral-segment models serve as another alternative that use to represent a more detailed spinal materials and geometries in studying the biomechanical behaviour of the spine (Rohlmann et al., 2006).

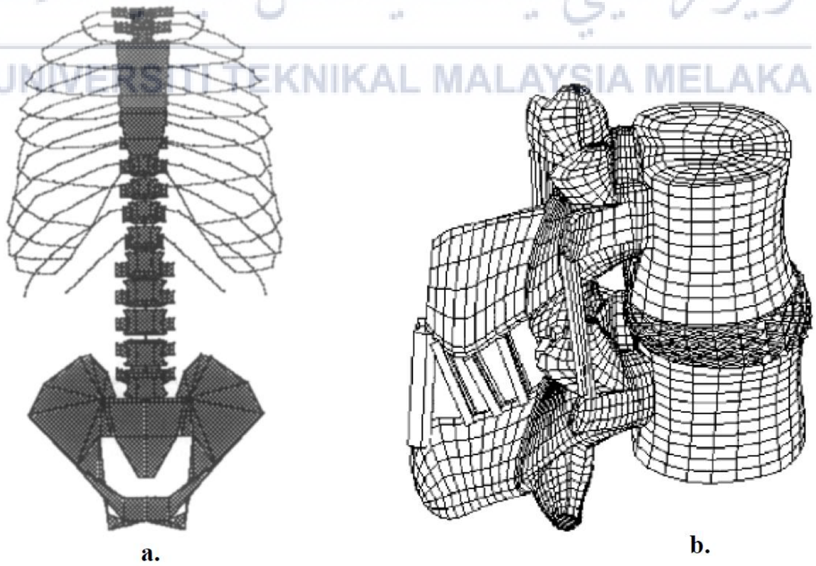

Figure 2.11: Two types of spine models a. Whole-spine model (Lee et al., 1995) b. Vertebral-segment model (Teo et al., 2004).

2.6.2 Finite element modelling of ligaments

The ligaments have been proved to bring crucial stabilizing effects to the spine and restrict the kinematics of spine. Therefore, it is important to implement ligaments in lumbar spine model to replicate a real spine and obtain reliable results ((Kim et al., 2014, Zahari et al., 2017, Pintar et al., 1992). However, ligaments are very complex to be modelled since CT scan is unavailable to retrieve their geometrical data. Therefore, alternatives such as 3D truss element are used to model ligaments without losing the reliability and their function (Kim et al., 2014, Zahari et al., 2017, Fan and Guo, 2018). The modelling of ligaments is shown in Figure 2.12.

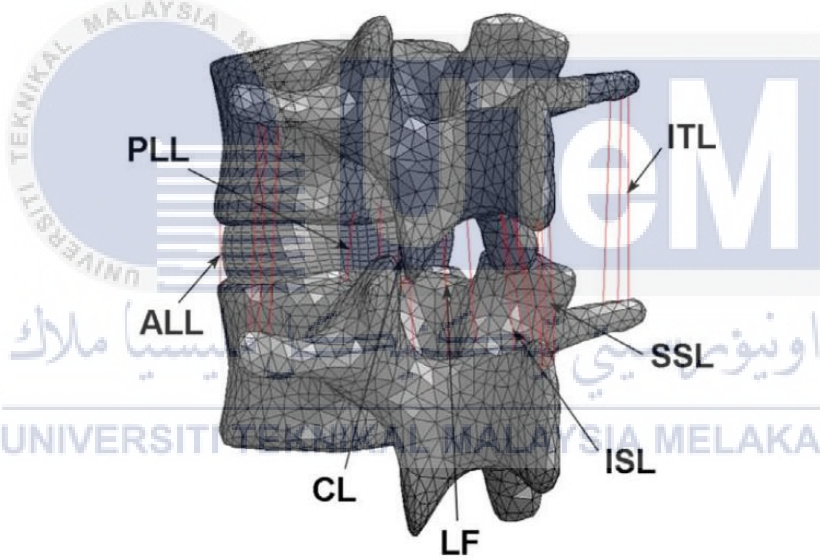

Figure 2.12: Models of ligament in truss element on FE lumbar spine (Fan and Guo, 2018).

2.6.3 Material properties of the human lumbar spine

The anterior vertebral body is composed of cortical bone and cancellous bone. The cortical bone is a thin and high dense shell which embeds the cancellous bone. The thickness of cortical bone used in modelling is normally 1.0mm (Zhang et al., 2018). Most of the studies applied isotropic material to define the biomechanical behaviour of bone structures in lumbar vertebrae (Schmidt et al., 2007, Zhang et al., 2018, Rohlmann et al., 2006).

In assigning material to intervertebral disc, since annulus fibrosus and nucleus pulposus are almost incompressible and do not perform linearly to the loading, Mooney-Rivlin constitutive model is mostly applied in previous studies to model their hyperelastic and incompressible behaviour (Schmidt et al., 2007, Park et al., 2013). In the meantime, non-linear criss-cross pattern truss element is mostly used in modelling the fibers of annulus (Park et al., 2013, Schmidt et al., 2007, Rohlmann et al., 2006)

The component used to model the facet joints are mostly the articular processes bone and cartilage layer. Most previous studies applied gap elements to define the space between two cartilage surfaces (Rohlmann et al., 2007) while some used surface to surface contact elements (Schmidt et al., 2007) and spring elements (Kim et al., 2014). Besides, frictionless sliding surface contact is mostly used between cartilage layers to model the synovial fluid effect at the facet joint (Kim et al., 2014, Schmidt et al., 2007).

To model the ligament attached at the lumbar vertebrae, truss element (Kim et al., 2014) and spring element (Schmidt et al., 2007) are mostly used with nonlinear material properties which show similar behaviour with a nonlinear stress-strain curve as shown in Figure 2.13.

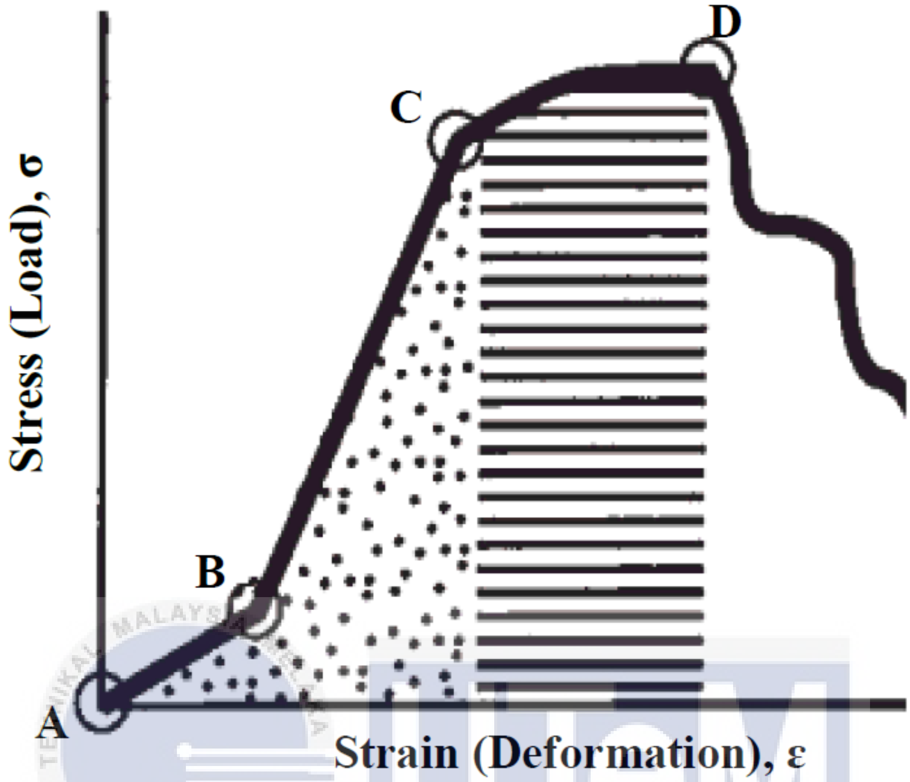

Figure 2.13: A common stress-strain curve for biological tissue. AB, the neutral zone; BC, the elastic zone. When the elastic limit (yield point C) is reached, permanent deformation can occur (permanent set). CD, the plastic zone where permanent set occurs. Past D, failure occurs, and the load diminishes. (Samandouras, 2010)

Table 2.1 showed the material properties used by previous study in modelling of human lumbar spine.

Table 2.1: The material properties used to model lumbar spine in previous studies.

Source	Cortical bone	Cancellous bone	Annulus fibrosus	Nucleus pulposus	Annulus fibers	Ligament	Cartilage of facet joint	Solver
Park et al. (2013)	E = 12,000 v= 0.3	E= 100 v= 0.2	Hyperelastic Mooney-Rivlin C_1= 0.18 C_2= 0.045	Incompressible fluid-filled cavity	Non-linear, depending on distance from disc center, 6 layers – criss-cross pattern	Non-linear stress-strain curve	Hard frictionless contact, E= 11 v= 0.4 Initial gap=0.5 mm	Abaqus 6.10
Ayturk and Puttlitz (2011)	E_{11} = 8,000 E_{22} = 8,000 E_{33} = 12,000 v_1 = 0.4 v_2 = 0.35 v_3 = 0.3	Based on CT images	Hyperelastic Yeoh C_{10} = 0.0146 C_{20} = -0.0189 C_{30} = 0.041	E = 1.0 v = 0.49	Non-linear, two families of fibers A_3 = 0.03 b_3 = 120.0 (unitless)	Exponential force-displacement curves	neo-Hookean	Abaqus 6.11
Schmidt et al. (2007)	E_1 = 22,000 E_2 = 11,300 v_1 = 0.484 v_2 = 0.203	E_1 = 200 E_2 = 140 v_1 = 0.45 v_2 = 0.315	Hyperelastic Mooney-Rivlin C_1 = 0.56 C_2 = 0.14	Incompressible fluid-filled cavity	Non-linear stress-strain curve, 16 layers – criss cross pattern	Non-linear stress-strain curve	Hard frictionless contact, E = 35 v = 0.4 Initial gap = 0.4 mm	Abaqus 6.10
Rohlmann et al. (2007)	E = 10,000 v = 0.3	E_1 = 200 E_2 =140 v_1 = 0.45	Hyperelastic Neo-Hookean C_1 = 0.3448	Incompressible fluid-filled cavity	Non-linear, dependant on distance form	Non-linear stress-strain curve	Soft frictionless contact,	Abaqus 6.10

		v_2 = 0.315	C_2 = 0.3		disc center, 14 layers – criss-cross pattern		Initial gap = 0.5 mm	
Kim et al. (2014)	E_1 = 22,000 E_2 = 11300 v_1 = 0.484 v_2 = 0.203	E_1 = 200 E_2 = 140 v_1 = 0.45 v_2 = 0.315	Elastic E = 4.2 v = 0.45	Incompressible fluid-filled cavity	Non-linear stress-strain curve, 8 layers criss-cross pattern	Non-linear stress strain curve	Hard frictionless contact, E = 35 v = 0.4 Initial gap = 0.5 mm	Abaqus 6.6
Du et al. (2016a)	E = 14,000 v = 0.3	E = 100 v = 0.2	Hyperelastic Mooney-Rivlin C_1 = 0.18 C_2 = 0.045	Hyperelastic Mooney-Rivlin C_1 = 0.12 C_2 = 0.03	Calibrated stress-strain curve	Calibrated deflection-force curves	Hyperelastic Neo-Hookean C_{10} = 2	Abaqus 6.11
Kurutz and Oroszvary (2010)	E = 12,000 v = 0.3	E = 150 v = 0.3	E = 4 v = 0.45 For tension, E = 0.4	E = 1 v = 0.499 For tension, E = 0.4	Tension only E = 500 for external fiber, 400 for middle fiber and 300 for internal fiber.	Linear elastic element, E = 8 for ALL E = 10 for PLL E = 5 for other ligaments,		ANSYS Classic

		v = 0.35 for all ligaments	

*E: Young's modulus (MPa); v: Poisson's ratio; C_1 and C_2: Material constant characterising the deviatoric deformation of material

2.6.4 Follower load method

Previous finite element analysis found that a small compressive load will significantly increase bending of lumbar spine, which may eventually cause buckling in spine even though the load intensity is way below that in vivo. These experiments were all using compressive vertical load at the superior surface of the spine and somehow when the critical load was exceeded, the spine become unstable and buckled (Crisco III, 1989, Lucas et al., 1961).

It was then in one study found that vertical compressive load may results in generating excessive bending moment, which cause the results unreliable. Therefore, to reduce the bending moment from being created, the resultant internal compressive load should be tangent to the curve of lumbar spine passing through the instantaneous centre of rotation of the lumbar segments as shown in Figure 2.14. This resultant internal compressive load is described as "follower load" which greatly reduce the excess bending moment. Therefore, this make the whole lumbar spine to support large compressive loads as seen in in vivo study (Patwardhan et al., 1999).

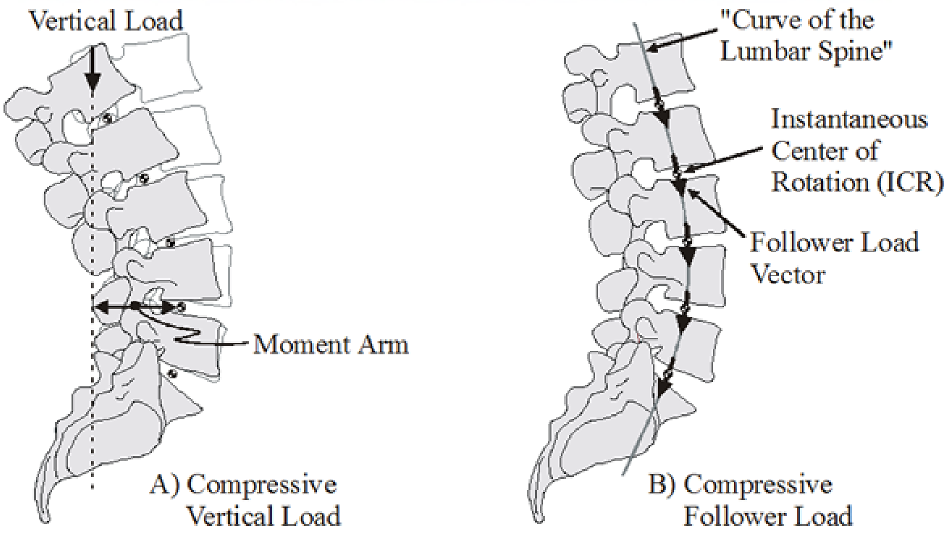

Figure 2.14: The application of (a) Compressive vertical load (b) Compressive follower load (Patwardhan et al., 1999)

2.6.5 Finite element studies of mechanical behaviour of human lumbar spine

A spinal motion segment is the functional spine unit (FSU) that shows the biomechanical behaviour of spine. It is comprised of two adjacent vertebrae, intervertebral disc and interconnecting ligaments (Olivier Y. Rolin). Each FSU exhibits six degree of freedom in rotation and translation. Rotational motions include flexion-extension, axial rotation and lateral bending; while translational motion include axial displacement, anterior shear and lateral shear. The ROM of the spine is restrict by constraints which depends on the posterior elements of the vertebrae such as the geometry and orientation of facet joints as shown in Figure 2.15 (Hall, 1991).

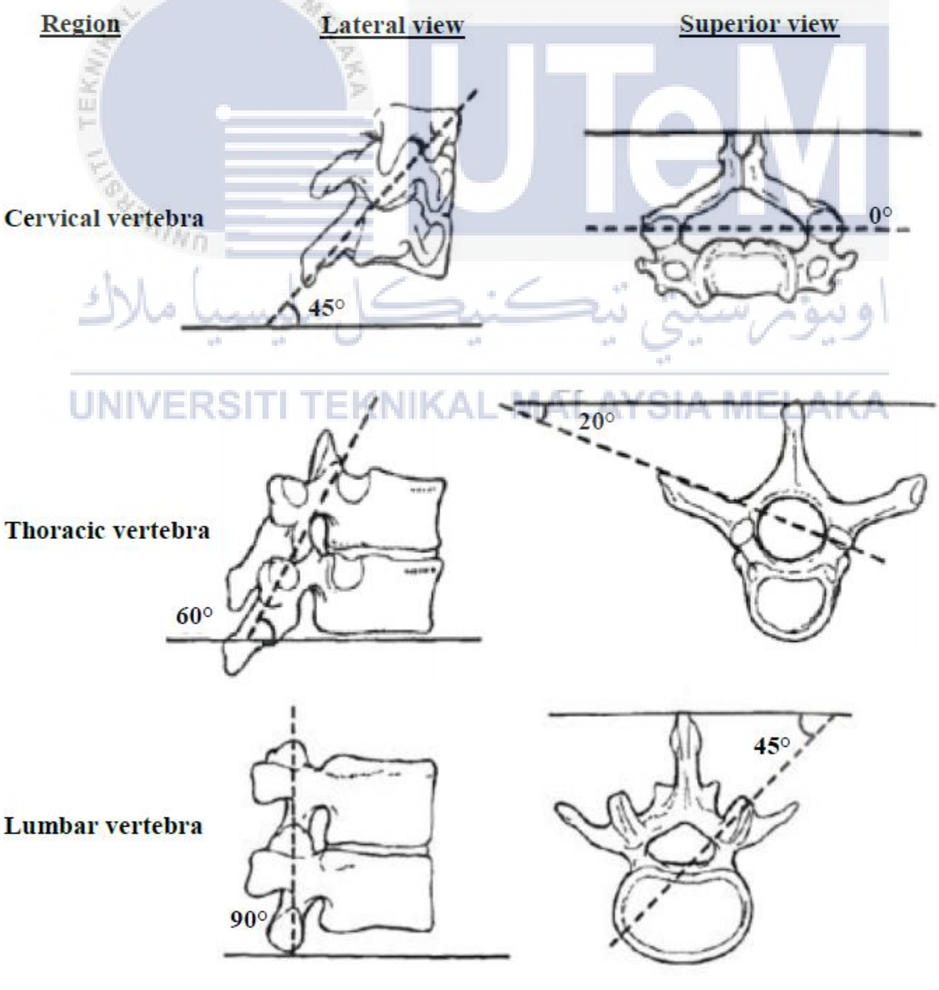

Figure 2.15: Orientation of facet joints (Hall, 1991).

2.6.6 Range of motion

Range of motion (ROM) is defined as the movement of joint measured in displacement or angle from its neutral position when loading is applied (Schulte et al., 2008). The range of motion is vital in study the physiological kinematics of the lumbar spine to understand its biomechanical behaviour. Through measurement of ROM we can also examine the stability of lumbar spine which is greatly related to low back pain (White and Panjabi, 1990, Panjabi, 2003). It is shown that increase in body weight can cause decrease in ROM of lumbar spine, which could cause muscular dystrophy that may eventually led to low back pain (Renner et al., 2007).

2.6.7 Intradiscal pressure of intervertebral disc

Intradiscal pressure (IDP) is the measure of hydrostatic pressure in the nucleus pulposus of IVD (Claus et al., 2008). Excessive mechanical loads are believed to induce high pressure at nucleus pulposus which might cause disc degeneration (Raj, 2008). The degenerated disc is proven as a cause of low back pain because its load-bearing behaviour has been altered (Urban and Roberts, 2003).

2.6.8 Stress analysis of the facet joint

Previous studies have shown that facet degeneration is highly related to occurrence of LBP (Jaumard et al., 2011b, Manchikanti et al., 2016, Gellhorn et al., 2013). A normal facet joint can transfer up to 25% of sagittal load in the spine. However, due to many reasons such as ageing, excessive mechanical load and genetic factors would cause degeneration of facet joint. This will cause the mechanical instability as the facet joint fails to maintain the motion of vertebrae, which in turn increases the mechanical stresses supported by the disc. When degeneration deteriorates, friction will occur at joints and eventually the articulating cartilage will wear off and erode which further reduce the function of facet joint. Results from previous studies has shown that increasing body weight will increase the contact stress at facet joints, thus increase the risk of facet degeneration and osteoarthritis that can cause low back pain (Du et al., 2016b, Jaumard et al., 2011a).

2.7 Research gap of knowledge

During normal activities, human lumbar spine shows crucial role in supporting the upper body. However, since it is frequently activated, there is high occurrence of disc and facet problems that may be arise from lots of reasons. One of the reasons is overweight and obese which greatly related to low back pain. This health disorder can be happened due to wide range of motion and stress at the lumbar spine and facet joint, especially for those who suffer overweight and obesity. Since the flexion-extension motions account for the largest ROM of lumbar spine, it is important to examine the effect of human weight on the biomechanical behaviour of spinal facet joints under these two motions.

CHAPTER 3

METHODOLOGY

3.1 Overview

The development of FE model of L1-L5 lumbar spine, including the vertebrae, intervertebral discs, facet joints and ligaments was presented. The FE model was verified by comparing the finite element analysis result with previous studies to prove that the FE model will behave and able to represent the behaviour the real model. Then, the verified model was subjected to different loading conditions to study the kinematics of spine, facet contact pressure and stress at capsular ligament.

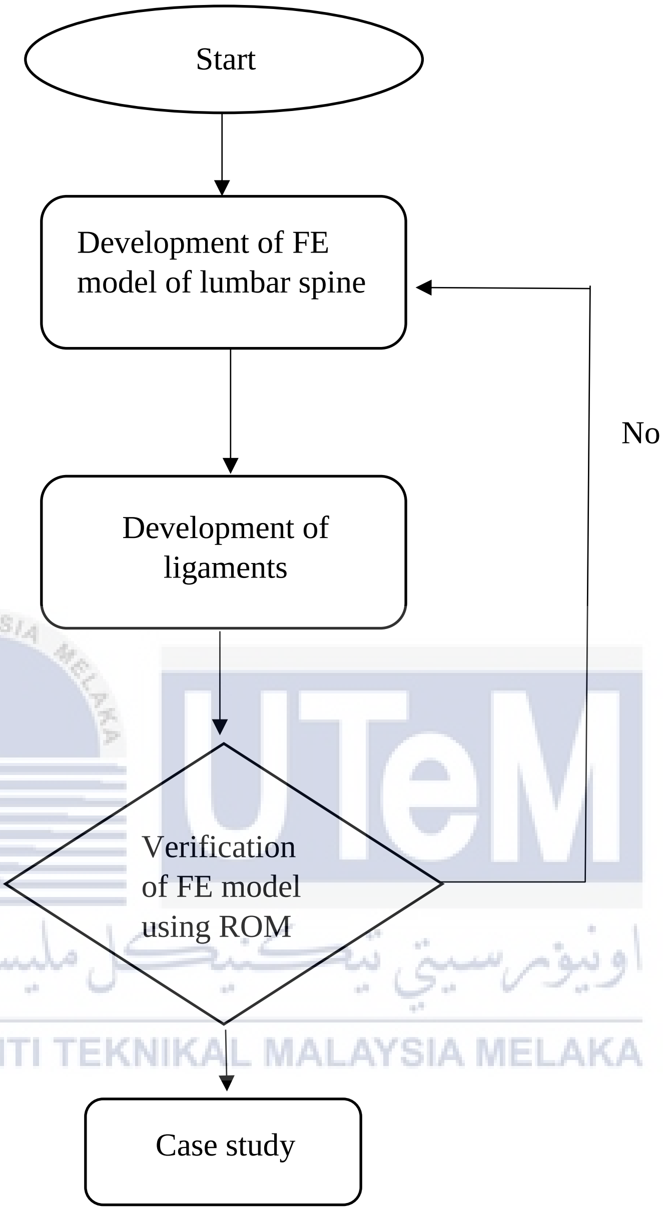

Figure 3.1: Methodology flow chart

3.2 Development of 3-D model of lumbar spine

The geometry of the L1-L5 lumbar spine was taken from the computer tomography (CT) scan of a healthy 23-year-old male volunteer, with a height of 1.73m and weight of 70kg with BMI of 23.39 kg/m^2. The data was obtained from Hospital Tengku Ampuan Afzan, Kuantan, Pahang, Malaysia as shown in Figure 3.1.

Figure 3.2: CT scan data of human spine

The segmentation of the vertebra bone images in each layer of the data was carried out to produce a Standard Tessellation Language (STL) format. Then, the 3-D model of the lumbar spine were generated using Mimics 14.0 software (Materialise, Leuven, Belgium) as shown in Figure 3.2.

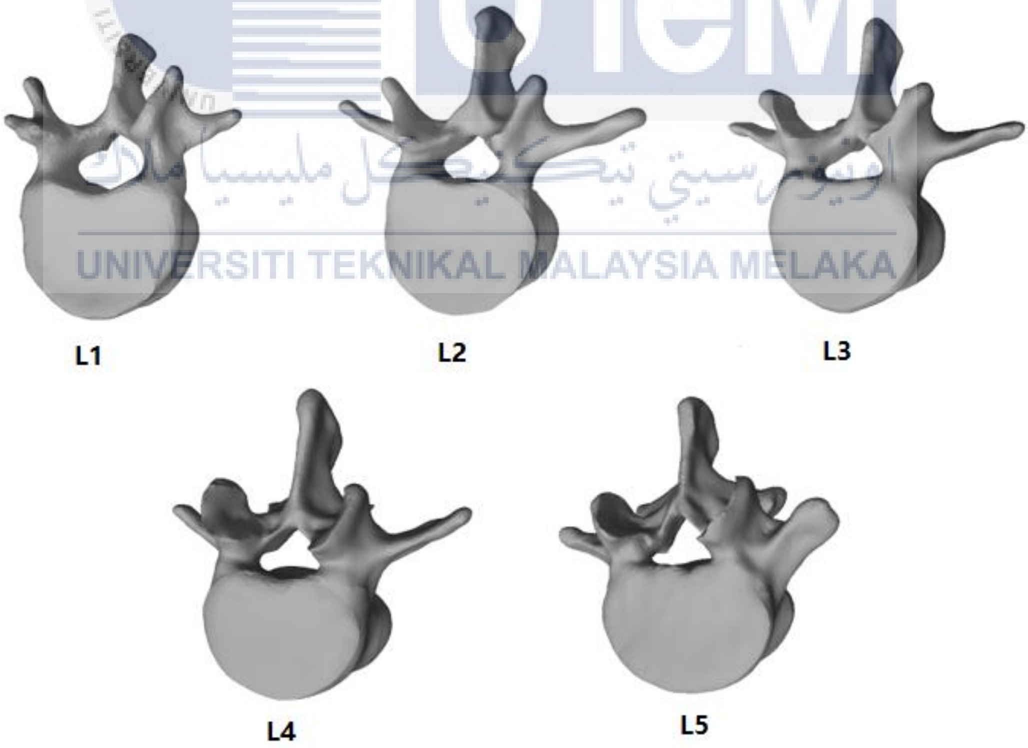

Figure 3.3: STL 3-D model of L1-L5 lumbar vertebrae.

The drawing of intervertebral discs and facet cartilage were obtained and modelled in Solidwork 2014 since CT scan could not retrieve image of soft tissues. The lumbar vertebrae are composed of a hard-cortical bone at outer layer and less dense cancellous bone inside. According to the data retrieved, the thickness of cortical bone was set to 1 mm and the thickness of cartilage tissue is 2 mm.

3.3 Finite element model of lumbar spine

The 3-D model was assembled, meshed and optimised using Abaqus. Simulation for case studies was also done using the same software to investigate the behaviour of lumbar spine. Figure 3.3 shows the 3-D FE model of the lumbar spine. There are total 1756884 tetrahedral elements and 355028 nodes in the lumbar spine model.

Figure 3.4: 3-D FE model of the lumbar spine

3.4 Material properties

The FE model was assigned with three sets of materials. For all models, linear and isotropic material properties were adopted for both the cortical and cancellous bones (Park et al., 2013, Zhang et al., 2018). The facet surfaces were made smooth to imitate the frictionless motion in real case. Besides, a gap of 0.5 mm between cartilage layers was set with linear and elastic properties (Kim et al., 2014). For components of intervertebral discs such as incompressible nucleus pulposus and hyperelastic annulus fibrosus, three types of materials were assigned to the models to compare the results. Moreover, tension only truss element was assigned to the annulus fibers with non-linear behaviour (Schmidt et al., 2007, Du et al., 2016a). The material properties for all three models were tabulated in Table 3.1 to Table 3.3.

Table 3.1: material properties used in the FE lumbar spine model 1.

Element Set	Materials Properties	Reference
Cortical bone	E = 12,000 MPa, v = 0.3	(Park et al., 2013)
Cancellous bone	E = 100 MPa, v = 0.2	(Park et al., 2013)
Articular cartilage	E = 35 MPa, v = 0.4	(Kim et al., 2014)
Annulus ground substance	E = 4.2 MPa, v = 0.45	(Schmidt et al., 2006)
Nucleus pulposus	E = 1.0 MPa, v = 0.4999	(Kim et al., 2014)

Table 3.2: material properties used in the FE lumbar spine model 2.

Element Set	Materials Properties	Reference
Cortical bone	E = 12,000 MPa, v = 0.3	(Park et al., 2013)
Cancellous bone	E = 100 MPa, v = 0.2	(Park et al., 2013)
Articular cartilage	E = 35 MPa, v = 0.4	(Kim et al., 2014)

Annulus ground substance	Mooney Rivlin: C1 = 0.18, C2 = 0.045	(Schmidt et al., 2007, Park et al., 2013)
Nucleus pulposus	Mooney Rivlin: C1 = 0.12, C2 = 0.03	(Schmidt et al., 2007)

Table 3.3: material properties used in the FE lumbar spine model 3.

Element Set	**Materials Properties**	**Reference**
Cortical bone	E = 12,000 MPa, v = 0.3	(Park et al., 2013)
Cancellous bone	E = 100 MPa, v = 0.2	(Park et al., 2013)
Articular cartilage	E = 11 MPa, v = 0.4	(Park et al., 2013)
Annulus ground substance	Mooney Rivlin: C1 = 0.42, C2 = 0.105	(Chen et al., 2001)
Nucleus pulposus	Mooney Rivlin: C1 = 0.12, C2 = 0.03	(Schmidt et al., 2007)

3.5 Development of Ligaments

3-D truss elements were used to model ligaments which only active in tension (Kim et al., 2014) as shown in Figure 3.5. The cross-sectional area of each ligament was taken from previous study as shown in Table 3.4.

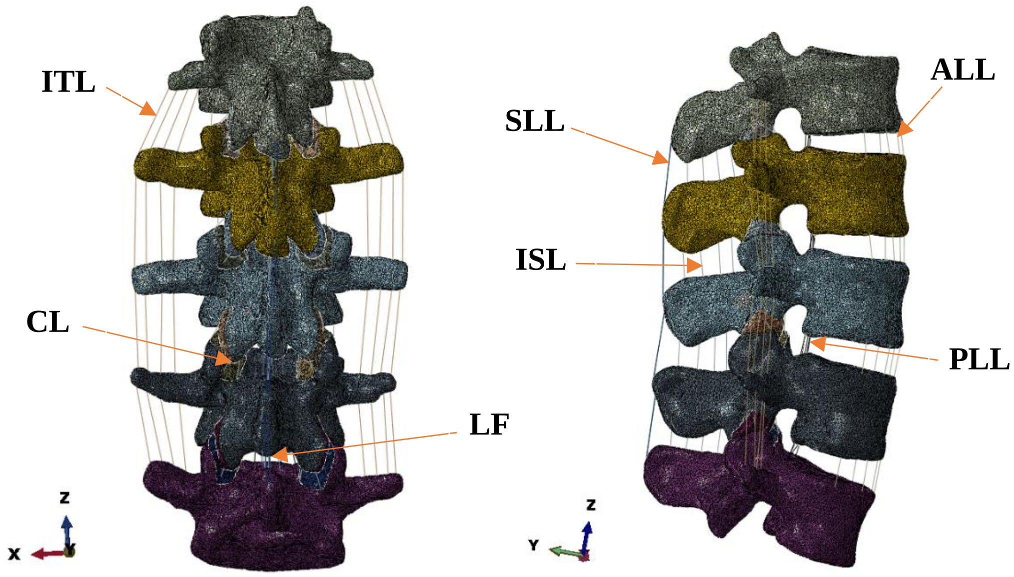

(a) (b)

Figure 3.5: FE modelling of the ligaments attached at the lumbar spine (a) posterior (b) lateral views

Table 3.4: Geometrical parameters of the lumbar spine ligaments.

Ligament	Cross sectional area (mm^2)	Reference
ALL	32.4	(Pintar et al., 1992)
PLL	5.2	(Pintar et al., 1992)
CL	1.46	(Zahari et al., 2014)
ITL	1.8	(Goel et al., 1995)
LF	10	(Pintar et al., 1992)
SSL	3	(Pintar et al., 1992)
ISL	11.6	(Zahari et al., 2014)

The ligaments were then modelled with 2 types of material properties to check whether which type worked perfectly in replicating the ligaments of real lumbar spine. Elastic material properties were assigned as type 1 while nonlinear material properties of the non-linear stress strain curve (Kim et al., 2014, Zahari et al., 2017) were assigned as type 2. The both types material properties for each ligament were shown in Table 3.5 and Table 3.6.

Table 3.5: Type 1 (elastic) material properties used for ligaments

Ligament	Material Properties	Reference
ALL	E = 20 MPa, *v* = 0.3	(Wang et al., 2016)
PLL	E = 70 MPa, *v* = 0.3	(Wang et al., 2016)
CL	E = 20 MPa, *v* = 0.3	(Wang et al., 2016)
ITL	E = 28 MPa, *v* = 0.3	(Wang et al., 2016)
LF	E = 50 MPa, *v* = 0.3	(Wang et al., 2016)
SSL	E = 28 MPa, *v* = 0.3	(Wang et al., 2016)
ISL	E = 28 MPa, *v* = 0.3	(Wang et al., 2016)

Table 3.6: Type 2 (nonlinear) material properties used for ligaments

Ligament	Material Properties	Reference
ALL	E = 7.8 MPa ($\varepsilon < 12\%$)	(Kim et al., 2014)
	E = 20 MPa ($\varepsilon > 12\%$)	(Zahari et al., 2017)
PLL	E = 10 MPa ($\varepsilon < 11\%$)	(Kim et al., 2014)
	E = 20 MPa ($\varepsilon > 11\%$)	(Zahari et al., 2017)
CL	E = 7.5 MPa ($\varepsilon < 25\%$)	(Kim et al., 2014)
	E = 32.9 MPa ($\varepsilon > 25\%$)	(Zahari et al., 2017)
ITL	E = 10 MPa ($\varepsilon < 18\%$)	(Kim et al., 2014)
	E = 58.7 MPa ($\varepsilon > 18\%$)	(Zahari et al., 2017)
LF	E = 15 MPa ($\varepsilon < 6.2\%$)	(Kim et al., 2014)
	E = 19.5 MPa ($\varepsilon > 6.2\%$)	(Zahari et al., 2017)
SSL	E = 8 MPa ($\varepsilon < 20\%$)	(Kim et al., 2014)
	E = 15 MPa ($\varepsilon > 20\%$)	(Zahari et al., 2017)
ISL	E = 10 MPa ($\varepsilon < 14\%$)	(Kim et al., 2014)
	E = 11.6 MPa ($\varepsilon > 14\%$)	(Zahari et al., 2017)

3.6 Loading and boundary condition

The caudal elements of L5 vertebrae were constrained in all directions. The contact surface between the vertebral bodies and the IVD was set to perfectly fit by using tied contact. The articulating facet surfaces were simulated as surface-to-surface contact using normal stiffness contact of 200 N/mm and friction coefficient of zero. A 7.5 Nm moment was applied to the superior surface of L1 to simulate flexion and extension as shown in figure 3.5. The moment was applied by using couple force acting on the anterosuperior and inferior superior of the L1 vertebra. The couple forces were calculated using equation of moment as shown in equation 3.1 (Nordin and Frankel, 2001) and presented in Table 3.2.

$$M = F_R \times d \quad (3.1)$$

Where M is the moment loads, F_R is the resultant force and d is the distance between anterior and posterior of the L1 vertebral body.

$$F_R = 7.5\ Nm \div 0.03m$$

$$F_R = 250N$$

$$F_R = \sqrt{F_y^2 + F_z^2}$$

Let $F_y = 0.3\ F_s$ (30% of force acting on y-axis);

$F_z = 0.7\ F_s$ (70% of force acting on z-axis)

Thus,

$$250N = \sqrt{(0.3\ F_s)^2 + (0.7\ F_s)^2}$$

$F_s = 328$ N

Hence,

$$F_y = 0.3 \ F_s = 0.3 \times 328 \ N = 98 \ N$$

$$F_z = 0.7 \ F_s = 0.7 \times 328 \ N = 230 \ N$$

Figure 3.6: Loading and boundary condition on lumbar spine model

Table 3.7: Magnitude of moment loading applied on lumbar spine model

Loading direction	**Anterior point**		**Posterior point**	
	F_y (N)	F_z (N)	F_y (N)	F_z (N)
Flexion	-98	-230	98	230
Extension	98	230	-98	-230

3.7 Verification of finite element model

Verification and validation are an important process to make sure credibility of the developed FE model is established and yield results with good accuracy for its specific use (Anderson et al., 2007). An unverified and invalidated FE model can lead to false conclusions as they give unproven system (Henninger et al., 2010). The result of in vitro study is taken to validate the accuracy that obtained for the movement of vertebrae to prove that the FE model is behaving normally.

3.7.1 Intersegmental rotations of the lumbar spine

The intersegmental rotations of lumbar spine models were calculated to verify its stability. The motions of FE models were compared with in vitro study under pure moments of 7.5 Nm for flexion and extension motions (Panjabi et al., 1994).

3.7.2 Intervertebral disc (IVD)

The IVD was verified by comparing the axial displacement and intradiscal pressure with previous *in vitro* study (Markolf and Morris, 1974, Ranu, 1990). A vertical compressive load of 1200N was applied to the superior vertebral body of L4 to represent pressure distribution and the inferior surface of L5 vertebral body was set as fixed with zero degree of freedom as shown in figure 3.6.

3.8 Finite element analysis of the lumbar spine model under different groups of human weight

In order to replicate lumbar flexion and extension, a combination of 7.5 Nm pure moments and compressive follower load was applied to the lumbar spine model. The compressive follower was applied using the follower load modelling technique shown in previous study (Patwardhan et al., 1999). The follower load was modelled based on the curvature of lumbar spine through the proximities of the instantaneous centre rotation (ICR) of the vertebral body. This will stabilize the lumbar spine by giving stiffening effect and give comparable effect of local muscles (Rohlmann et al., 2001). Besides, it can avoid the FE model from generating unnecessary moments and thus increase the load capacity of the lumbar spine.

The compressive load represents the upper body weight subjected to lumbar vertebrae which is equal to about 60% of body weight with an additional muscle force approximately equal to the upper body weight (Rohlmann et al., 2001, Kurutz and Oroszváry, 2010). The selection of weights for normal, overweight and obese was calculated based on BMI at height 1.73m which was the height of the volunteer. Therefore, weight of 55 kg, 80kg and 110 kg were imposed for normal weight, overweight and obese, respectively. Therefore, the compressive follower load of 700N, 900N and 1300N were used in this study.

CHAPTER 4

RESULTS AND DISCUSSION

4.1 Overview

This chapter revealed and discussed the results gained from the simulation of FE lumbar spine model. The L1-L5 FE lumbar spine models were verified based on the range of motion, intradiscal pressure and axial displacement of intervertebral disc with *in vitro* study results. Then, intersegmental rotation of lumbar vertebrae, facet contact pressure and stress at capsular ligament during flexion and extension were studied.

4.2 The effects of ligaments in lumbar spine model

The verification of the FE lumbar spine models was performed based on the intersegmental rotations, Intervertebral disc axial displacement and intradiscal pressure. The verification is crucial in order to obtain reliable results while making sure the FE model is able to replicate the behaviour of human lumbar spine.

4.2.1 Intersegmental rotations of the lumbar spine model

The FE model of lumbar spine was verified by comparing the ROM with previous *in vitro* study for flexion and extension under pure moment of 7.5 Nm (Panjabi et al., 1994). Generally, the results of these models shown similar trend of ROM compared with previous *in vitro* study. However, for model 2 there was about 35.63% difference in flexion motion comparing with the *in vitro* result while there was 103.16% difference in extension motion under pure moment up to 7.5 Nm. Model 3 showed better result which there was only 20.58% difference in flexion and 27.03% difference in extension at moment of 7.5 Nm. The model 1 showed maximum 45.27% difference in flexion at 2.5 Nm and 40% for extension at – 2.5 Nm.

The graphs of range of motion against moment applied were plotted for L1-L5 in Figure 4.1.

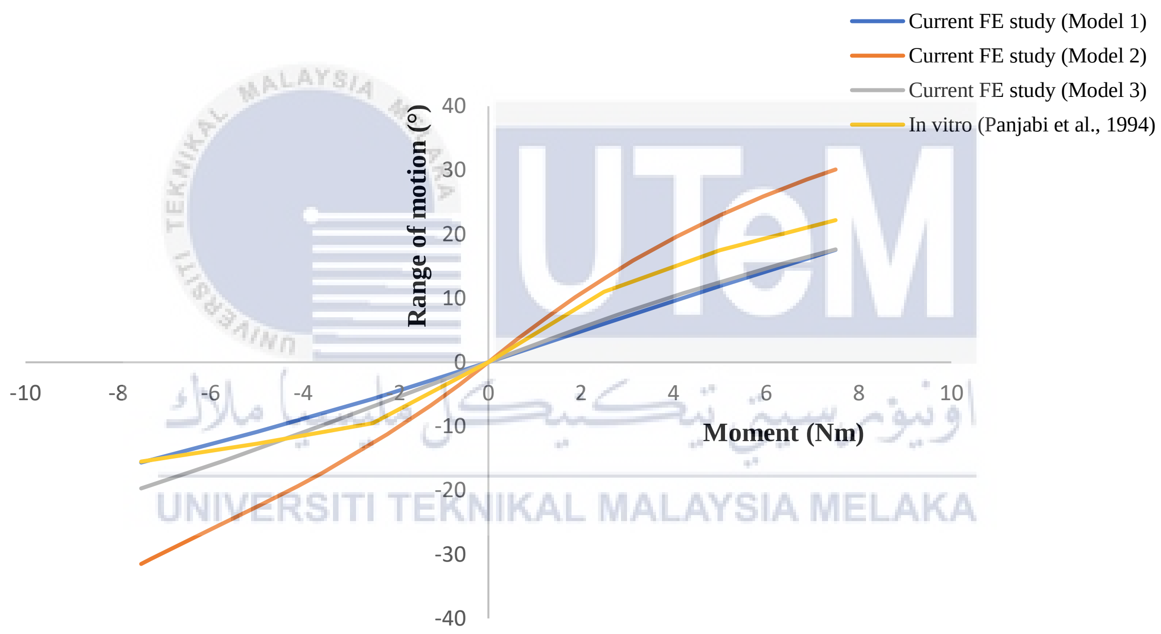

Figure 4.1: The comparison of total ROM of the lumbar spine between FE models and previous in vitro result (Panjabi et al., 1994) under pure moment from -7.5 Nm to 7.5Nm.

For both model 2 and 3, the ROM obtained showed deviation from experimental results because hyperelastic materials were assigned to the models which permitted greater flexibility. Besides, lack of modelling of ligaments also influenced the ROM since ligaments will constraint the kinematics of spine (Zander et al., 2004).

In short, since modelling of ligaments will constraint the flexibility of lumbar spine. Therefore, Model 2 will used for further ligaments modelling as this model had followed the trend as *in vitro* study with great ROM that can be constraint by using ligaments.

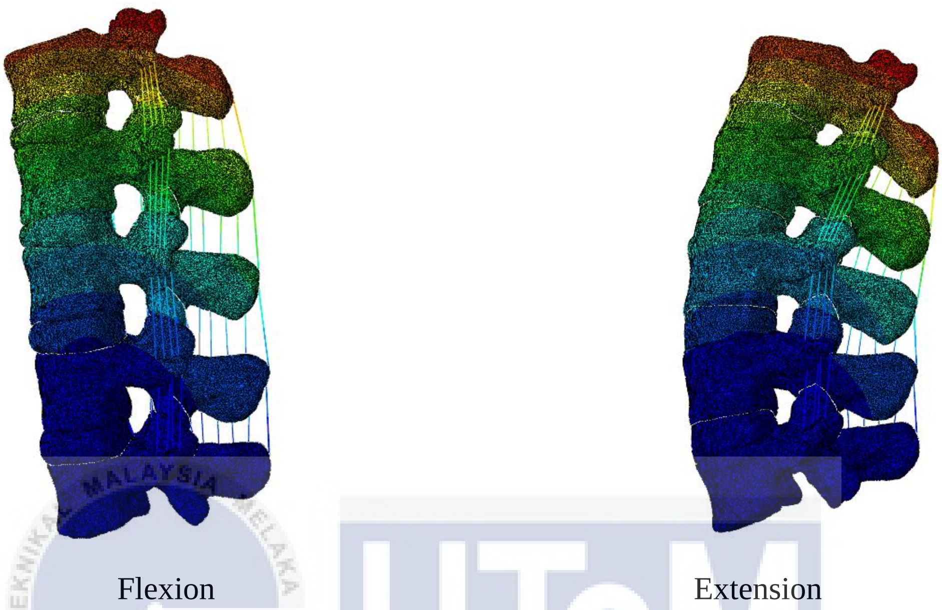

Figure 4.2: Deformation of lumbar spine model under flexion and extension rotation

4.2.2 Intersegmental rotation of lumbar spine model with ligaments

Ligaments with elastic properties were modelled to the lumbar spine model and verified again with *in vitro* study. The comparison results for intersegmental rotation was plotted in Figure 4.3. The maximum difference for lumbar spine with elastic ligament under flexion was about 19.75% at 7.5Nm while maximum difference under extension was 65.5% at -7.5 Nm. Therefore, it was concluded that further improvement needed to be done to improve the accuracy of lumbar spine FE model.

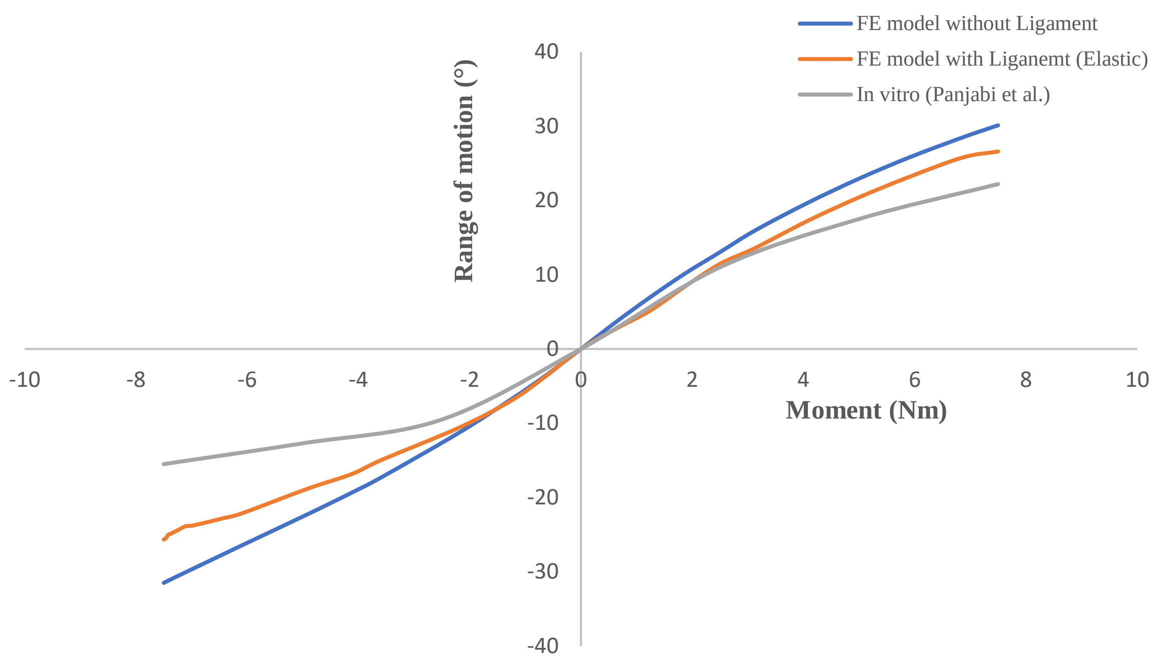

Figure 4.3: The comparison of total ROM of the lumbar spine between FE models (with elastic ligaments and without ligaments) and previous in vitro result (Panjabi et al., 1994) under pure moment from -7.5Nm to 7.5Nm.

4.2.3 Intervertebral disc (IVD)

The axial displacement and intradiscal pressure (IDP) of the FE lumbar spine model was compared with previous *in vitro* studies as shown in Figure 4.4 (Markolf and Morris, 1974, Ranu, 1990). The maximum percentage difference for axial displacement were 59.72% for FE model without ligaments and 59.77% for FE model with ligaments under compressive load at 1200N. Meanwhile, the maximum percentage difference for IDP were 29.21% for FE model without ligaments and 63.96% for FE model with ligaments under compressive load at 1200N. Therefore, these results further concluded that improvement needed to be done in order for FE lumbar spine model to replicate real lumbar spine.

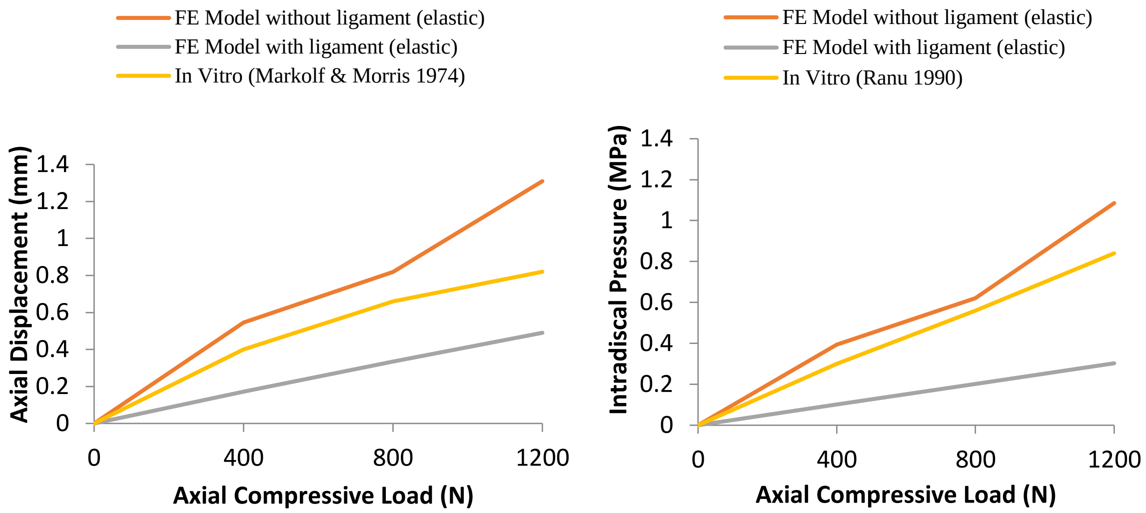

(a) (b)

Figure 4.4: Comparison of present FE Model (with and without elastic ligaments) and previous *in vitro* studies of the IVD results (a) axial displacement (b) intradiscal pressure under compressive load up to 1200N.

4.3 Verification of human lumbar spine FE model with hyperelastic ligaments

The verification of the FE lumbar spine model with complete ligaments modelled was performed based on the intersegmental rotations, Intervertebral disc axial displacement and intradiscal pressure. The verification is crucial to obtain reliable results while making sure the FE model was able to replicate the behaviour of human lumbar spine. Besides, this verification will prove that hyperelastic properties were better than elastic properties in modelling of ligaments.

4.3.1 Intersegmental rotation of lumbar spine model with hyperelastic ligaments

Verification of FE lumbar spine model with ligaments under hyperelastic properties was done by comparing the intersegmental rotation with previous *in vitro* study (Panjabi et al., 1994) as shown in Figure 4.5. The maximum percentage differences for flexion was 9.1% at 7.5Nm while for extension was 3.95% at -7.5Nm. Thus, it was concluded that the FE lumbar spine model with hyperelastic ligaments was able to replicate the real lumbar spine and produce reliable result in further studies.

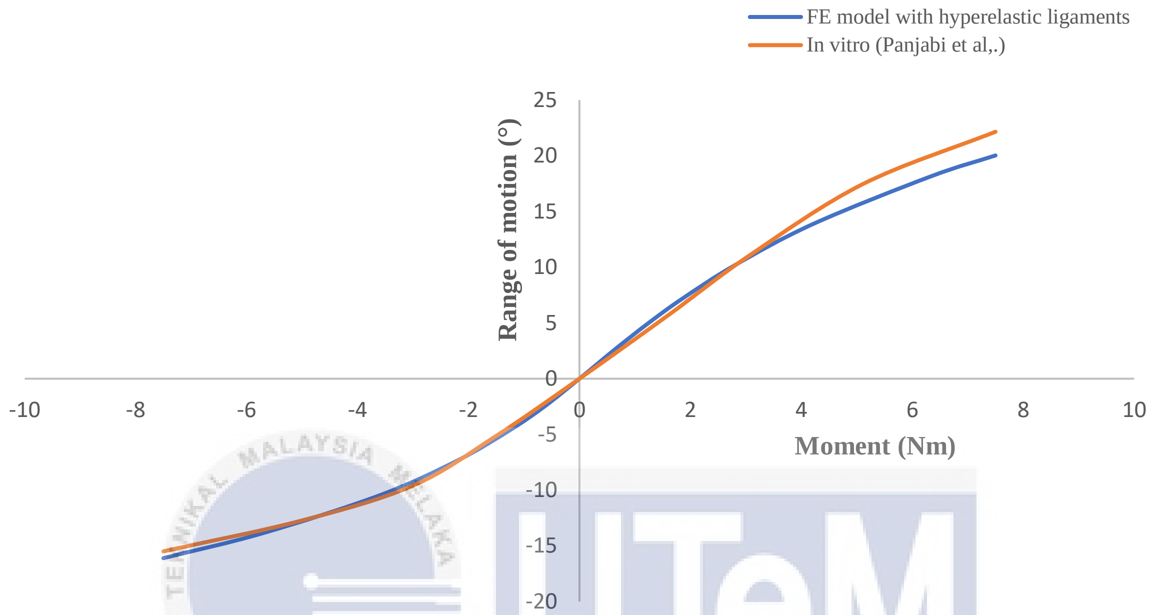

Figure 4.5: The comparison of total ROM of the lumbar spine between FE models (with hyperelastic ligaments) in vitro result (Panjabi et al., 1994) under pure moment from -7.5Nm to 7.5Nm.

4.3.2 Intervertebral disc verification with hyperelastic ligaments modelled

The axial displacement and intradiscal pressure (IDP) of the FE lumbar spine model with hyperelastic ligaments was compared with previous *in vitro* studies as shown in Figure 4.6 (Markolf and Morris, 1974, Ranu, 1990). The maximum percentage difference for axial displacement was 10.2% under compressive load at 1200N. Meanwhile, the maximum percentage difference for IDP was 16.8% under compressive load at 400N. The result of IDP and axial displacement showed almost similar trend with previous *in vitro* studies (Markolf and Morris, 1974, Ranu, 1990). Therefore, these results showed that the FE model was able to produce reliable results for further analysis.

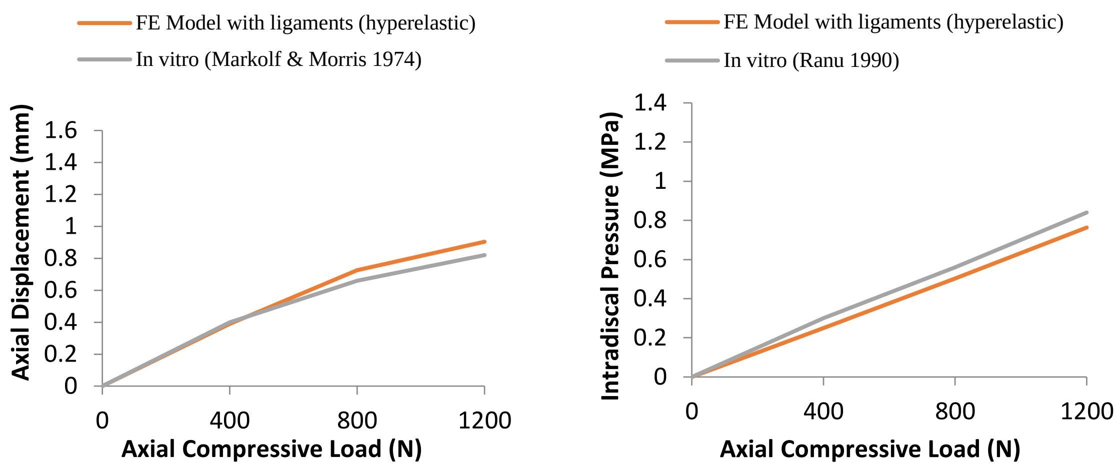

(a) (b)

Figure 4.6: Comparison of present FE Model (hyperelastic ligaments) and previous *in vitro* studies of the IVD results (a) axial displacement (b) intradiscal pressure under compressive load up to 1200N.

4.4 Biomechanical effects of human weight on FE lumbar spine model

The verified FE lumbar spine model was used to evaluate the biomechanical effects of normal, overweight and obese on the kinematics of lumbar spine, facet contact pressure and stress at capsular ligaments.

4.4.1 The effects of human weight on the kinematics of lumbar spine

The FE lumbar spine model was subjected to normal, overweight and obese loading condition to examine the kinematics of lumbar spine. The result of simulation shown that the human weight will affect the kinematics of lumbar spine. The intersegmental rotations of lumbar spine for flexion and extension under different loading conditions were shown in Figure 4.7.

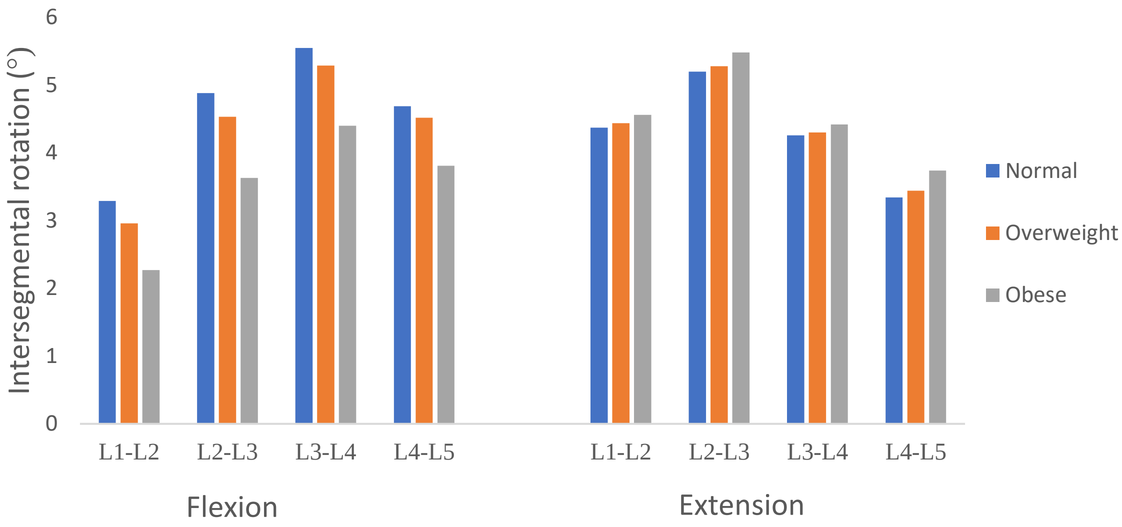

Figure 4.7: Intersegmental rotation for normal, overweight and obese under flexion and extension motion.

It was shown that the intersegmental rotation of lumbar spine decreased with increasing compressive load for flexion. However, in extension there was an opposite trend where the intersegmental rotation increased with increasing compressive load. Therefore, it was proved that human weight will affect the kinematics of lumbar spine. This was also found in previous *in vitro* study where the compressive load affected the intersegmental rotation of lumbar spine in both flexion and rotation motions (Patwardhan et al., 1999).

From the results, it was found that the percentage difference of intersegmental rotation between normal weight and obese under flexion was much higher than it was under extension. The intersegmental rotation under flexion showed an average decrease of 24% from normal weight to obese while the intersegmental rotation under extension showed an average increase of 6.37% from normal weight to obese. The maximum percentage difference for intersegmental rotation under flexion was 31% happened at L1-L2 vertebrae while maximum percentage difference for intersegmental rotation under extension was 11.97%

happened at L4-L5 vertebrae. Overall, it is shown that the increasing compressive load would decrease the total intersegmental rotation of flexion-extension motion as shown in Figure 4.8.

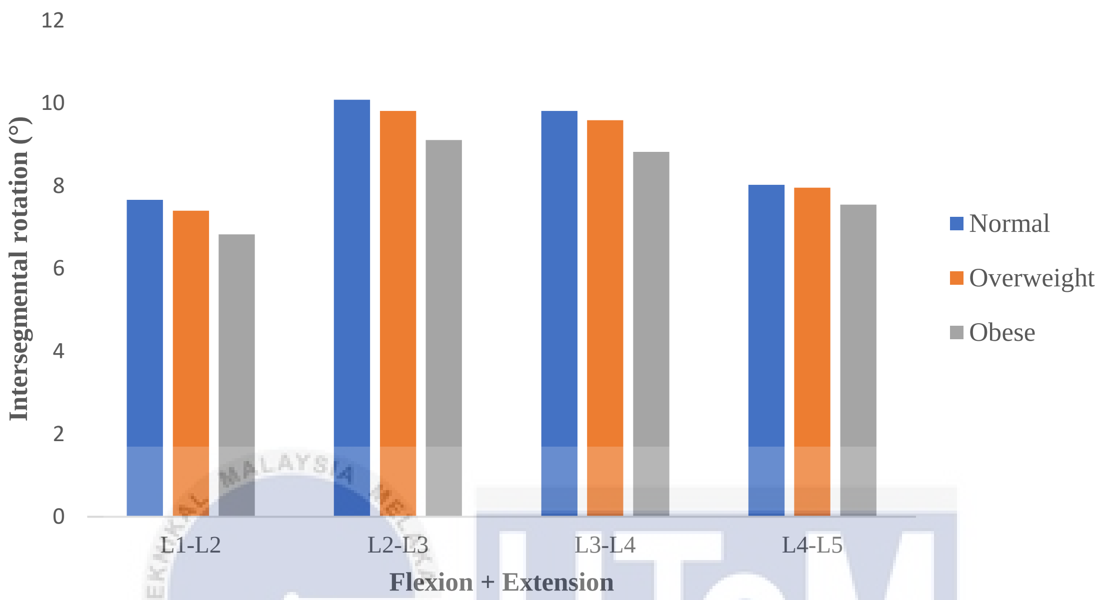

Figure 4.8: Intersegmental rotation for flexion-extension under normal, overweight and obese load.

The results of this study could explain the association of LBP among obese people. A clinical study has found that obesity could reduce intersegmental rotation of lumbar spine for flexion-extension motion which tally with present study where excessive weight tend to stiffen the lumbar spine which restrict motion. In the same time, previous study also found that the reduced intersegmental rotation was highly associated with LBP which further proved that obesity would cause low back pain (Vismara et al., 2010).

4.4.2 The effects of human weight on the stress at capsular ligament

In the investigation of effect of human weight on stress at capsular ligament, only extension motion of lumbar spine was focused since the flexion motion did not affect much to the stress at capsular ligament (Chen et al., 2014). The stresses at capsular ligament for all three loading under extension motion were shown in Figure 4.9.

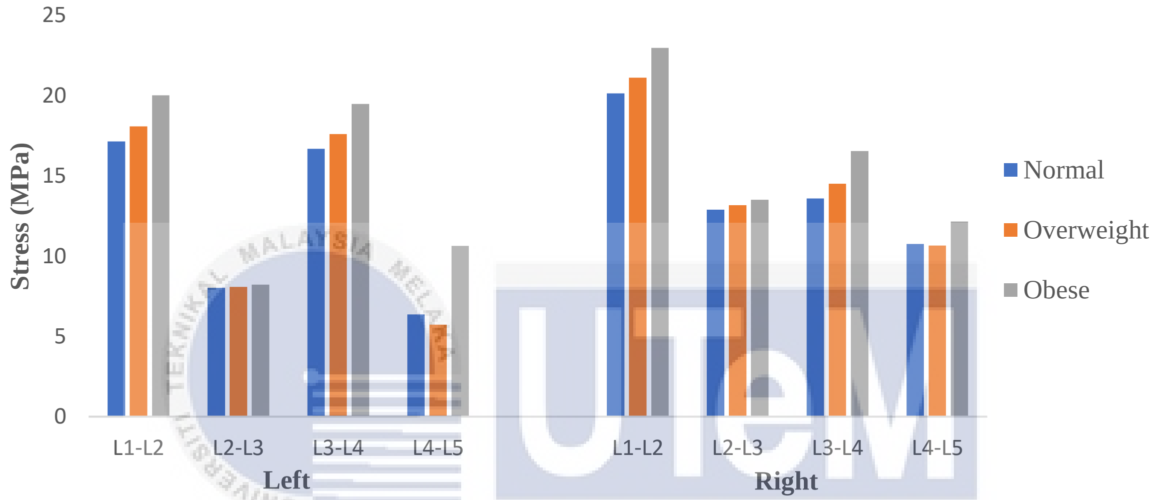

Figure 4.9: Stress at capsular ligament

From the result, it showed that there was a trend which the stress at capsular ligament increased with increasing loads. The results also indicated that the stresses of capsular ligament were slightly different. This was due to asymmetry behaviour of the facet joint and it was found to be appear in many of the previous studies (Kuo et al., 2010, Du et al., 2016a). The maximum percentage of stress increased at left capsular ligament was 66.75% between L4-L5 vertebrae. In the meantime, the maximum percentage of stress increased at right capsular ligament was 12.43% between L1-L2 vertebrae. The increasing stress at capsular ligament would stimulate the nociceptor nerve surrounding capsule which would cause low back pain (Chen et al., 2014).

4.4.3 The effects of human weight on the facet contact pressure

The contact pressure on the facet surfaces for all three loading cases under flexion and extension motions were presented in Figure 4.10, Figure 4.11, Figure 4.12 and Figure 4.13 while the pressure distributions on the facet surfaces for flexion and extension under normal weight and obese weight were presented in Figure 4.14, Figure 4.15, Figure 4.16 and Figure 4.17.

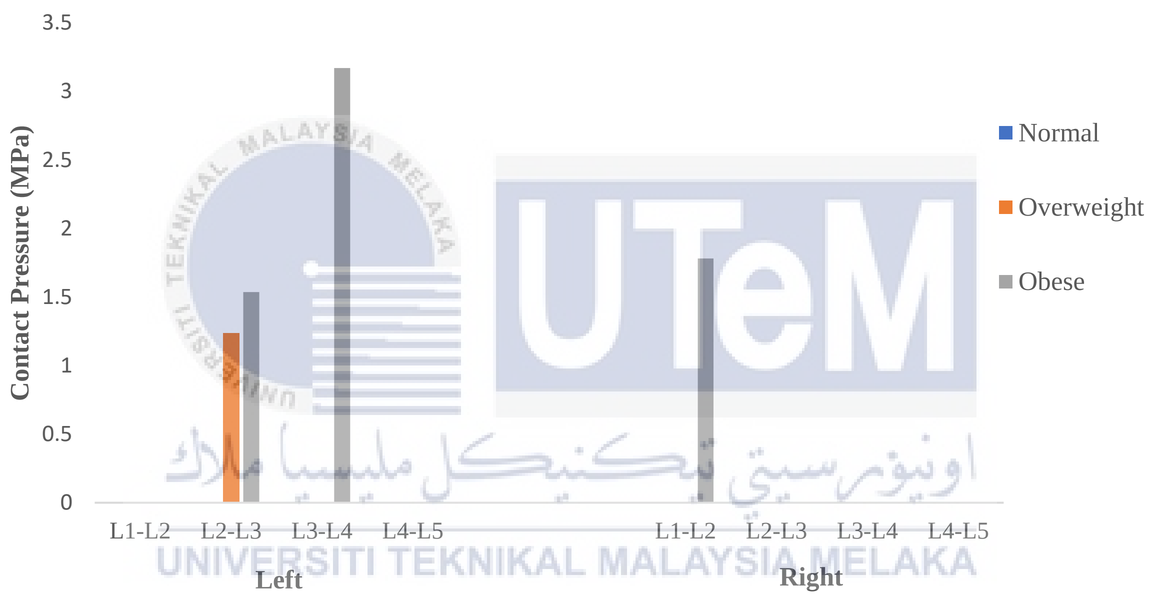

Figure 4.10: Left and right inferior facet contact pressure under flexion motion.

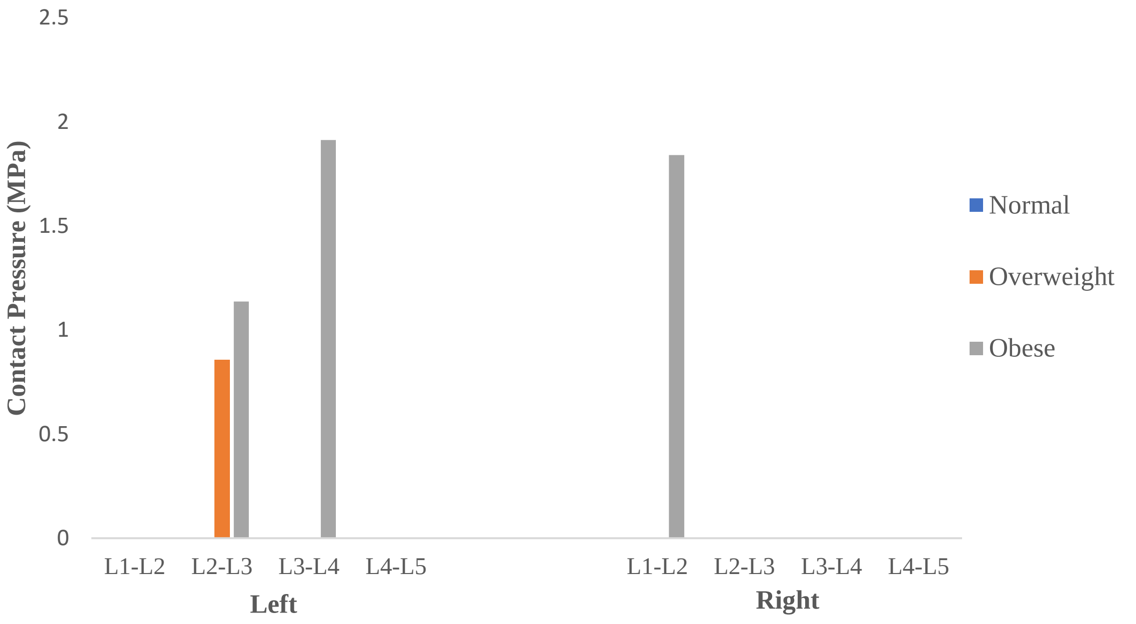

Figure 4.11: Left and right superior facet contact pressure under flexion motion.

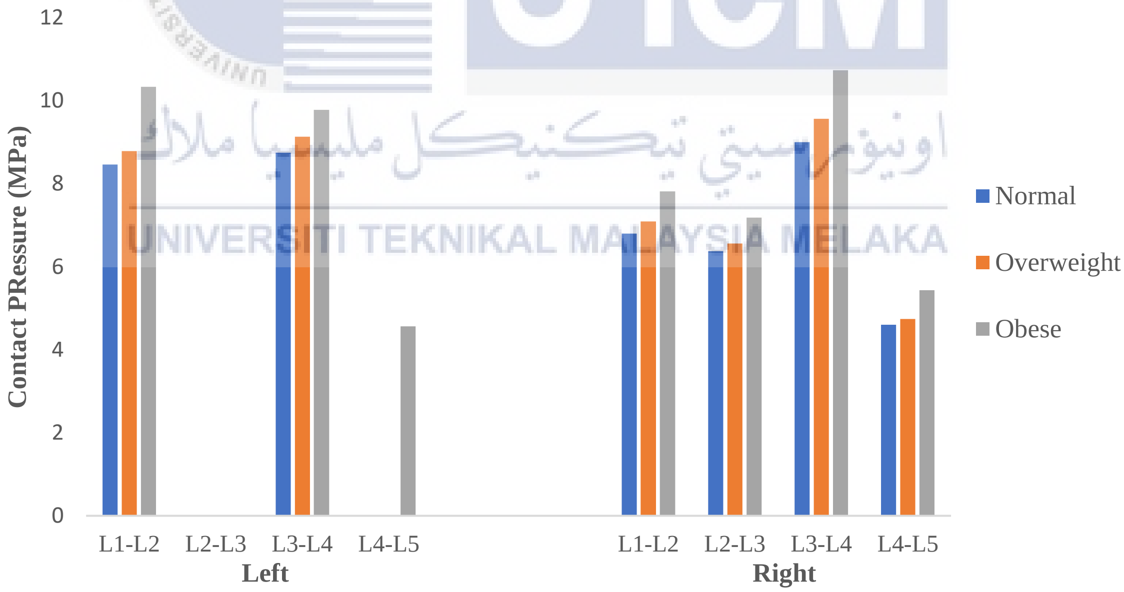

Figure 4.12: Left and right inferior facet contact pressure under extension motion

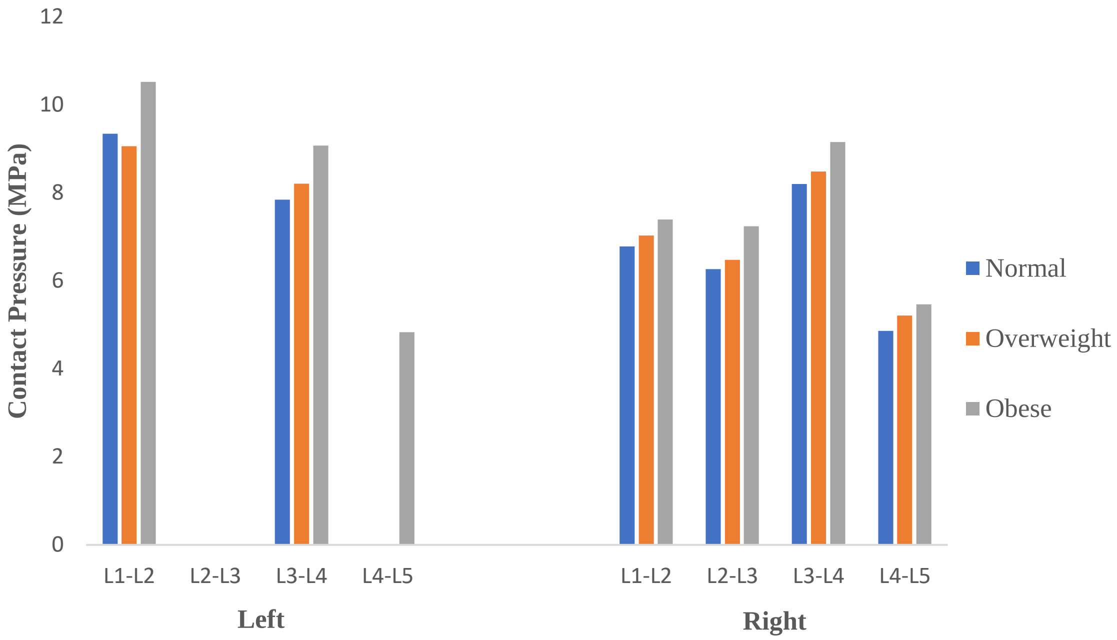

Figure 4.13: Left and right superior facet contact pressure under extension motion

During flexion motion, the two adjacent facets in lumbar vertebrae are supposed to move further from each other and do not create contact pressure (Du et al., 2016b, Jaumard et al., 2011a). This has been shown Figure 4.10 and Figure 4.11 where there was no contact pressure in flexion under normal weight condition. Based on the results, it has shown that there was asymmetry behaviour of facet joint where the stress did not generate at both left and right facets at some level. This asymmetry problem was due to the reason that the spine was not perfectly symmetrical and it was found to appear in most of the previous study (Du et al., 2016b, Jaumard et al., 2011a, Kuo et al., 2010)

It was found that the facet contact pressure increased with load for both flexion and extension motion. It was also shown that in obese condition, facet contact pressure became existed in flexion motion. In extension motion, the highest left facet contact pressure happened at facet surfaces at L1-L2 of lumbar spine while highest right facet contact pressure happened at facet surfaces at L3-L4 of lumbar spine.

In extension, there was an average of 16.96% increment of left inferior facet contact pressure from normal weight to obese while the highest increment of left inferior facet contact pressure happened at L4-L5 facet surfaces with 4.56 MPa increase. The right inferior facet contact pressure showed average 16.21% increment while the highest increment happened at L3-L4 facet surfaces. At the same time, the left and right superior facet contact pressure showed average pressure increment of 14.19% and 12.16% respectively. The highest superior facet contact pressure was 15.53% at right L2-L3 facet surfaces and from 0 to 4.83 MPa at left L4-L5 facet surfaces.

Based on the results obtained, it clearly showed that obesity would cause increase in facet contact stress which can cause several health problems such as osteoarthritis and facet degeneration. This could eventually lead to low back pain or even severe low back pain (Dreyer and Dreyfuss, 1996, Kalichman and Hunter, 2007).

	Left		Right	
	Inferior (Bottom)	Superior (Top)	Inferior (bottom)	Superior (Top)
L1-L2	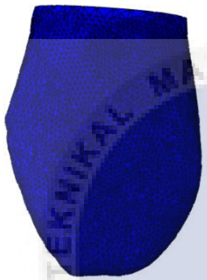	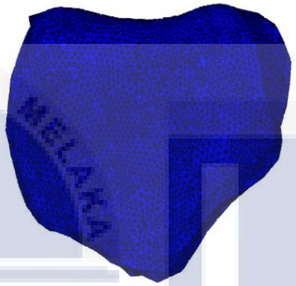	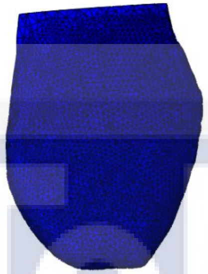	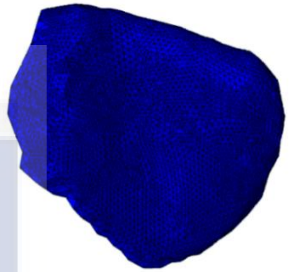
L2-L3			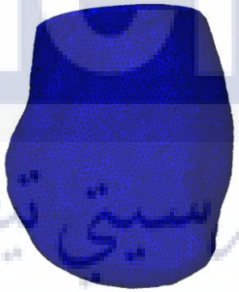	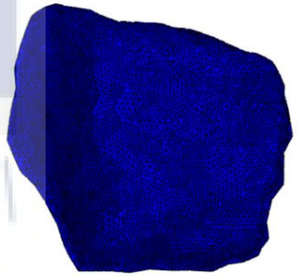
L3-L4	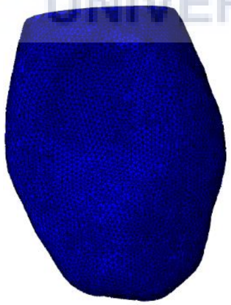		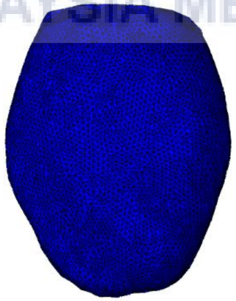	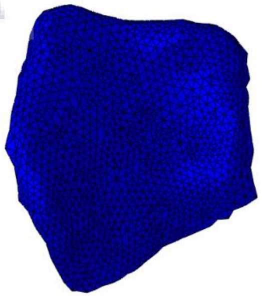

L4-L5	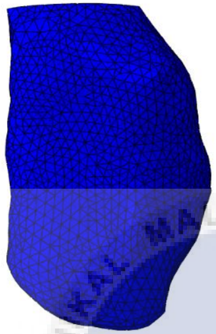	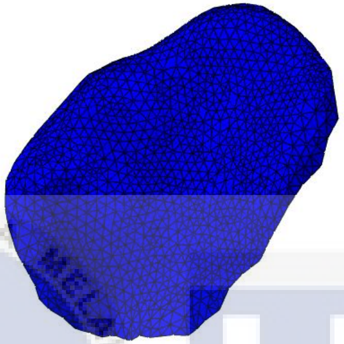	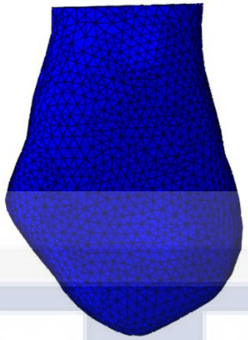	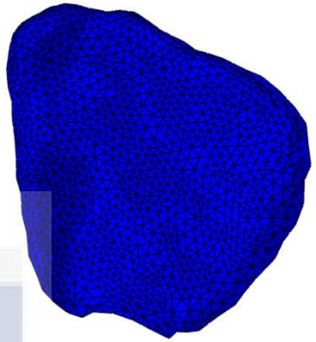

Figure 4.14: Pressure distribution for flexion under normal weight

	Left		Right	
	Inferior (Bottom)	Superior (Top)	Inferior (bottom)	Superior (Top)
L1-L2				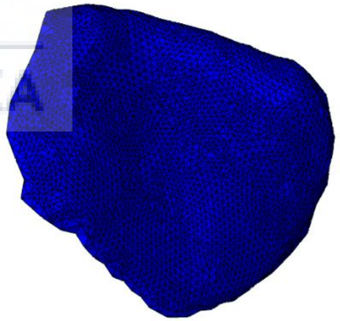

L2-L3	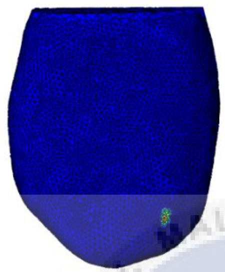	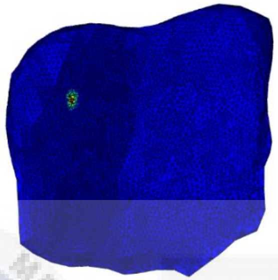	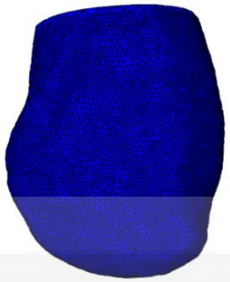	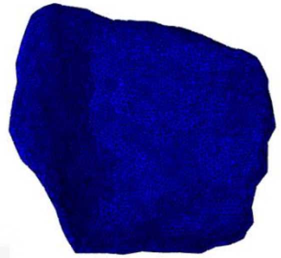
L3-L4	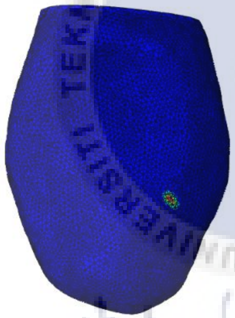	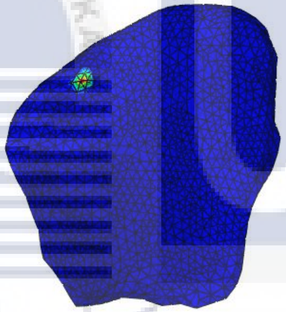		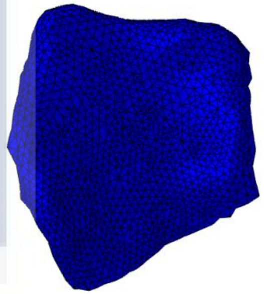
L4-L5				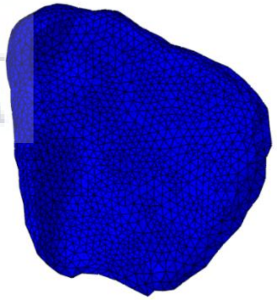

Figure 4.15: Pressure distribution for flexion under obese weight

	Left		Right	
	Inferior (Bottom)	Superior (Top)	Inferior (bottom)	Superior (Top)
L1-L2	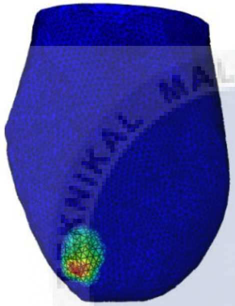	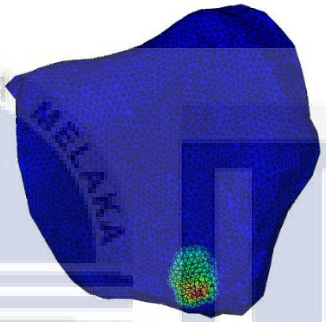	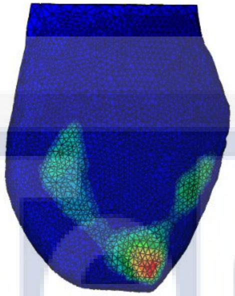	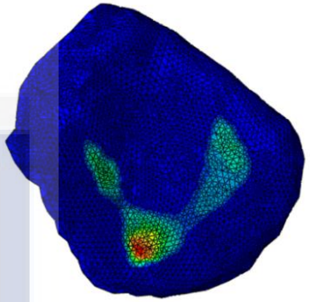
L2-L3		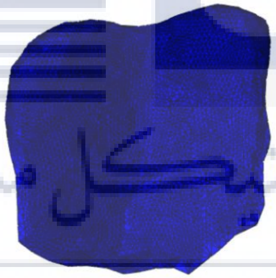	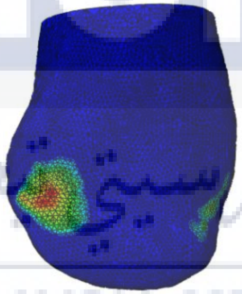	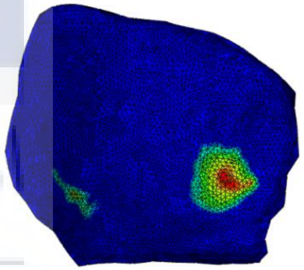
L3-L4	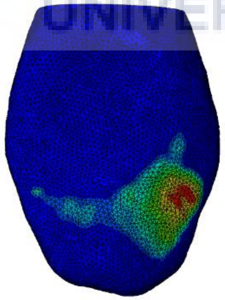	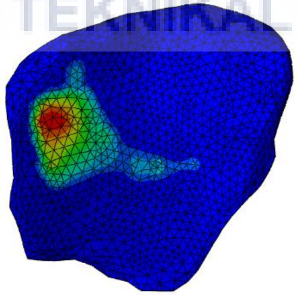	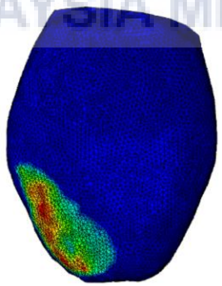	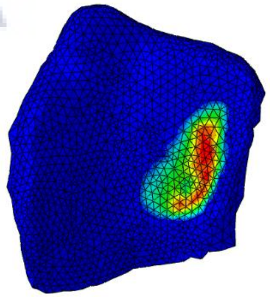

L4-L5	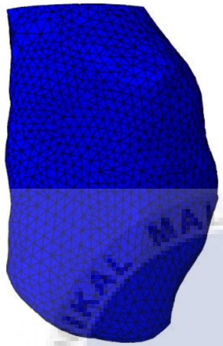	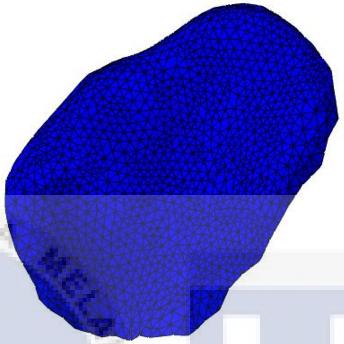	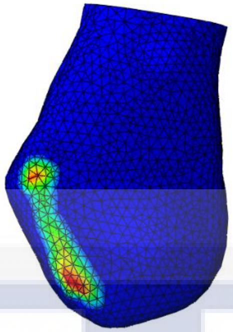	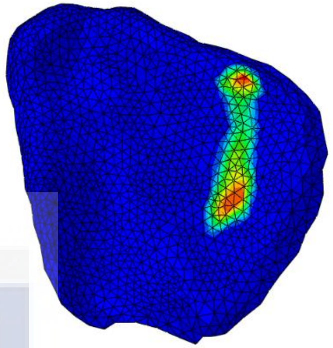

Figure 4.16: Pressure distribution for extension under normal weight

	Left		Right	
	Inferior (Bottom)	Superior (Top)	Inferior (bottom)	Superior (Top)
L1-L2	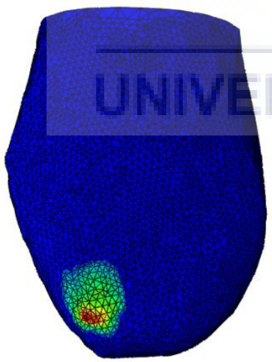	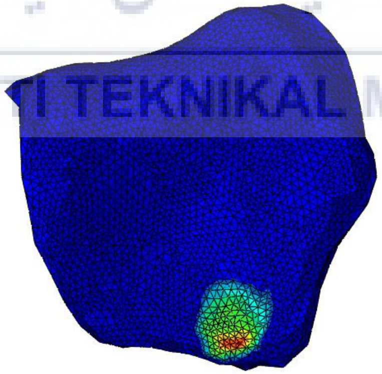	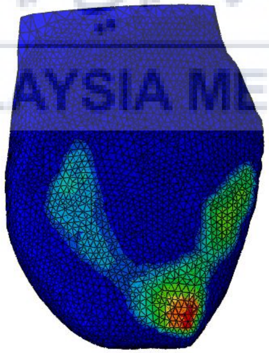	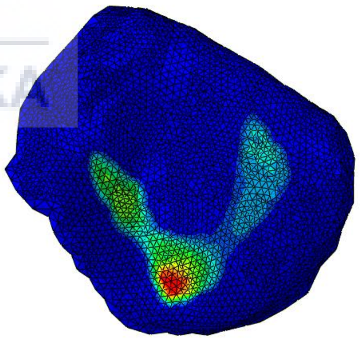

L2-L3	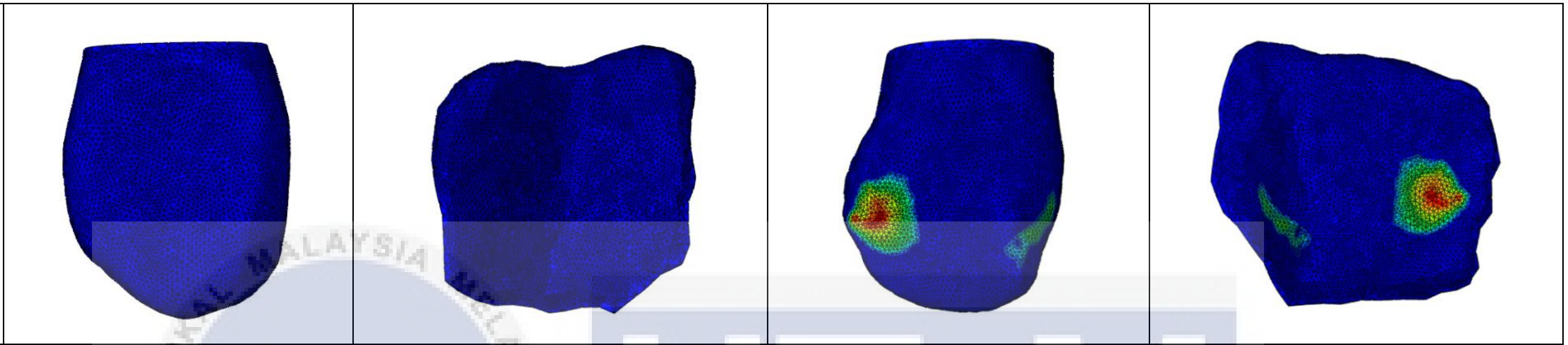
L3-L4	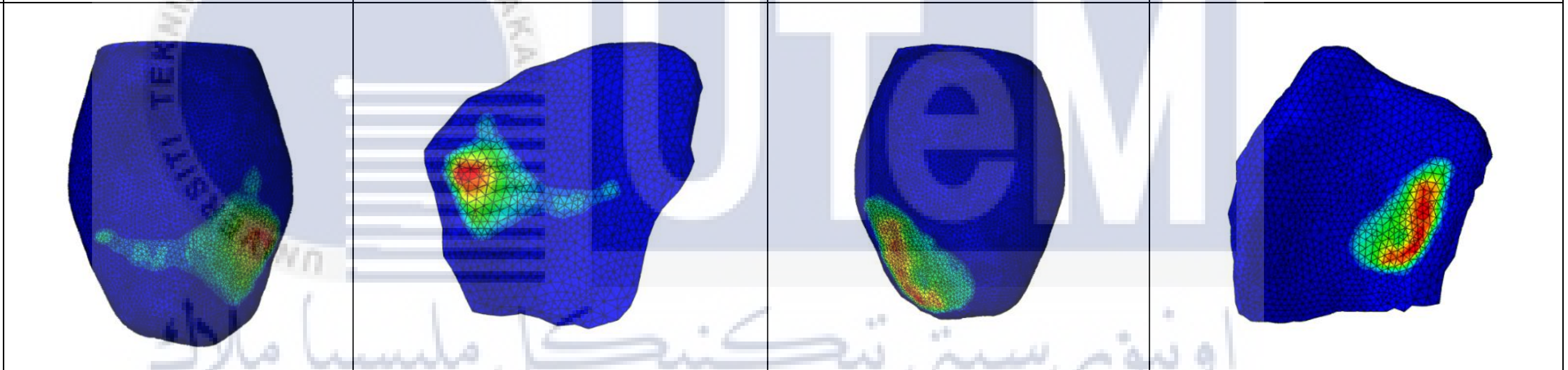
L4-L5	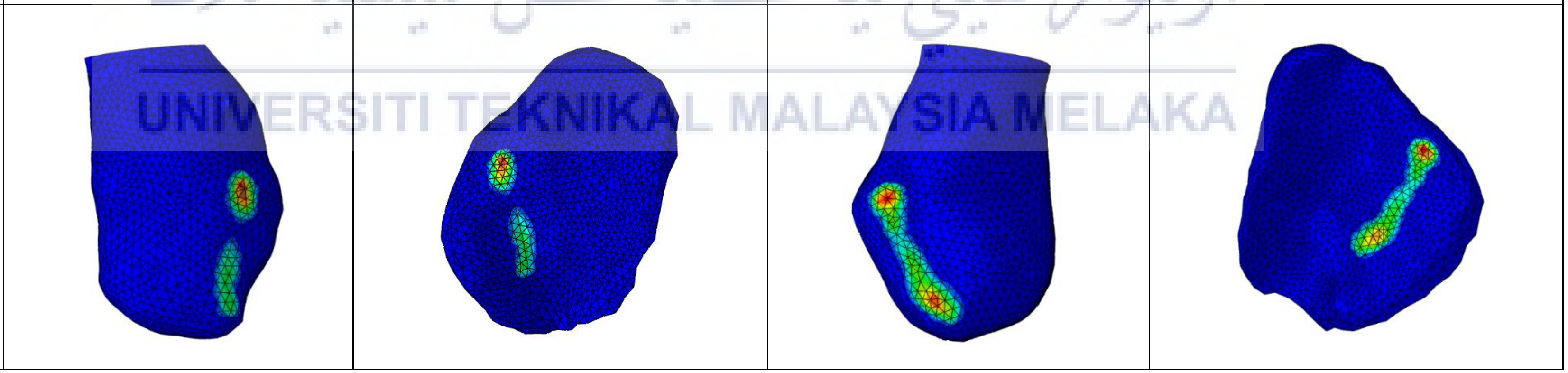

Figure 4.17: Pressure distribution for extension under obese weight

CHAPTER 5

CONCLUSION AND RECOMMENDATION FOR FUTURE RESEARCH

5.1 Conclusion

This project had developed a verified FE lumbar spine which able to replicate the biomechanical behaviour of real spine. It was used to investigate the effects of human weight on the kinematics of the lumbar spine, facet contact pressure and stress at capsular ligament.

The results showed that obesity caused maximum 31% reduced in intersegmental rotations under flexion and about 12% reduced range of motion for flexion-extension motion. Moreover, there was maximum 66.75% of stress increased at capsular ligament between L4-L5 vertebrae. It also showed increasing trend for facet contact pressure where the contact pressure increased as load increased.

It was proved that the kinematics of lumbar spine as well as facet contact pressure and stress at capsular ligament were affected by increasing human weight. Increasing weight would cause decreased flexibility of lumbar spine and eventually results in low back pain. Besides, excess facet contact pressure would build up with increasing loads from body weight which could eventually cause facet degeneration and osteoarthritis. Increased in stress at capsular ligament due to obesity would also stimulate surrounding nociceptor which induces pain at lower back area.

5.2 Recommendations for future research

There are several assumptions considered in the modelling and analysis of the lumbar spine that was subjected to various loading. In this study, the analysis was done based on computational methodology, which reminded that present study is non biological experiment and thus biological factors such as ageing and genetic factor were not considered during the analysis. Besides, the soft tissue, muscle and fat was not considered in present study. These limitations may provide false accuracy and therefore limit the simulation of true clinical scenario.

This study could be extended further into using three-dimensional model for ligaments as well as annulus fibres to investigate its mechanical behaviour under different loading for more reliable result. Other aspects that should be considered in future studies include the effects of human weight on the intervertebral disc of lumbar spine and under various kind of motions such as lateral bending and axial torsion.

REFERENCE

Anderson, A. E., Ellis, B. J. & Weiss, J. A. 2007. Verification, validation and sensitivity studies in computational biomechanics. *Comput Methods Biomech Biomed Engin,* 10**,** 171-84.

Ayturk, U. M. & Puttlitz, C. M. 2011. Parametric convergence sensitivity and validation of a finite element model of the human lumbar spine. *Comput Methods Biomech Biomed Engin,* 14**,** 695-705.

Balagué, F., Mannion, A. F., Pellisé, F. & Cedraschi, C. 2012. Non-specific low back pain. *The Lancet,* 379**,** 482-491.

Bergmark, A. 2009. Stability of the lumbar spine. *Acta Orthopaedica Scandinavica,* 60**,** 1-54.

Bogduk, N. 2005. *Clinical anatomy of the lumbar spine and sacrum / Nikolai Bogduk ; foreword by Stepen M. Endres,* New York, Churchill Livingstone.

Bray, R. C., Salo, P. T., Lo, I. K., Ackermann, P., Rattner, J. B. & Hart, D. A. 2005. Normal ligament structure, physiology and function. *Sports Medicine and Arthroscopy Review*.

Chen, C.-S., Cheng, C.-K., Liu, C.-L. & Lo, W.-H. 2001. Stress analysis of the disc adjacent to interbody fusion in lumbar spine. *Medical Engineering & Physics*.

Chen, H. L., Guo, K. J., Yuan, F. & Ding, N. 2014. Effect of stress on intervertebral disc and facet joint of novel lumbar spine soft implant: Biomechanical analysis. *Biomedical Research (India)*.

Claus, A., Hides, J., Moseley, G. L. & Hodges, P. 2008. Sitting versus standing: does the intradiscal pressure cause disc degeneration or low back pain? *J Electromyogr Kinesiol,* 18**,** 550-8.

Crisco Iii, J. J. 1989. The biomechanical stability of the human lumbar spine: Experimental and theoretical investigations. *ProQuest Dissertations and Theses*.

Devereaux, M. W. 2007. Anatomy and examination of the spine. *Neurol Clin,* 25**,** 331-51.

Deyo, R. A. 1992. What Can the History and Physical Examination Tell Us About Low Back Pain? *JAMA: The Journal of the American Medical Association,* 268.

Dreyer, S. J. & Dreyfuss, P. H. 1996. Low back pain and the zygapophysial (facet) joints. *Archives of Physical Medicine and Rehabilitation,* 77**,** 290-300.

Du, C. F., Yang, N., Guo, J. C., Huang, Y. P. & Zhang, C. 2016a. Biomechanical response of lumbar facet joints under follower preload: a finite element study. *BMC Musculoskelet Disord,* 17**,** 126.

Du, C. F., Yang, N., Guo, J. C., Huang, Y. P. & Zhang, C. 2016b. Biomechanical response of lumbar facet joints under follower preload: A finite element study. *BMC Musculoskeletal Disorders*.

Ebraheim, N. A., Hassan, A., Lee, M. & Xu, R. 2004. Functional anatomy of the lumbar spine. *Seminars in Pain Medicine.*

Fan, W. & Guo, L. X. 2018. Finite element investigation of the effect of nucleus removal on vibration characteristics of the lumbar spine under a compressive follower preload. *Journal of the Mechanical Behavior of Biomedical Materials*.

Flegal, K. M., Kit, B. K., Orpana, H. & Graubard, B. I. 2013. Association of all-cause mortality with overweight and obesity using standard body mass index categories: a systematic review and meta-analysis. *JAMA,* 309**,** 71-82.

Fujiwara, A., Lim, T. H., An, H. S., Tanaka, N., Jeon, C. H., Andersson, G. B. J. & Haughton, V. M. 2000. The effect of disc degeneration and facet joint osteoarthritis on the segmental flexibility of the lumbar spine. *Spine*.

Gellhorn, A. C., Katz, J. N. & Suri, P. 2013. Osteoarthritis of the spine: the facet joints. *Nat Rev Rheumatol,* 9**,** 216-24.

Goel, V. K., Kong, W., Han, J. S., Weinstein, J. N. & Gilbertson, L. G. 1993. A Combined Finite Element and Optimization Investigation of Lumbar Spine Mechanics With and Without Muscles. *Spine,* 18**,** 1531-1541.

Goel, V. K., Monroe, B. T., Gilbertson, L. G. & Brinckmann, P. 1995. Interlaminar shear stresses and laminae separation in a disc: Finite element analysis of the l3-l4 motion segment subjected to axial compressive loads. *Spine*.

Hall, S. J. 1991. *The biomechanics of the human spine*.

Han, K. S., Rohlmann, A., Yang, S. J., Kim, B. S. & Lim, T. H. 2011. Spinal muscles can create compressive follower loads in the lumbar spine in a neutral standing posture. *Med Eng Phys,* 33**,** 472-8.

Hartvigsen, J., Hancock, M. J., Kongsted, A., Louw, Q., Ferreira, M. L., Genevay, S., Hoy, D., Karppinen, J., Pransky, G., Sieper, J., Smeets, R. J., Underwood, M., Buchbinder, R., Cherkin, D., Foster, N. E., Maher, C. G., Van Tulder, M., Anema, J. R., Chou, R., Cohen, S. P., Menezes Costa, L., Croft, P., Ferreira, M., Ferreira, P. H., Fritz, J. M., Gross, D. P., Koes, B. W., Öberg, B., Peul, W. C., Schoene, M., Turner, J. A. & Woolf, A. 2018. What low back pain is and why we need to pay attention. *The Lancet*.

Henninger, H. B., Reese, S. P., Anderson, A. E. & Weiss, J. A. 2010. Validation of computational models in biomechanics. *Proc Inst Mech Eng H,* 224**,** 801-12.

Jaumard, N. V., Bauman, J. A., Weisshaar, C. L., Guarino, B. B., Welch, W. C. & Winkelstein, B. A. 2011a. Contact Pressure in the Facet Joint During Sagittal Bending of the Cadaveric Cervical Spine. *Journal of Biomechanical Engineering*.

Jaumard, N. V., Welch, W. C. & Winkelstein, B. A. 2011b. Spinal facet joint biomechanics and mechanotransduction in normal, injury and degenerative conditions. *J Biomech Eng,* 133, 071010.

Kalichman, L. & Hunter, D. J. 2007. Lumbar facet joint osteoarthritis: a review. *Semin Arthritis Rheum,* 37, 69-80.

Kim, H. J., Kang, K. T., Chang, B. S., Lee, C. K., Kim, J. W. & Yeom, J. S. 2014. Biomechanical analysis of fusion segment rigidity upon stress at both the fusion and adjacent segments: a comparison between unilateral and bilateral pedicle screw fixation. *Yonsei Med J,* 55, 1386-94.

Koes, B. W., Van Tulder, M. W. & Thomas, S. 2006. Diagnosis and treatment of low back pain. *BMJ,* 332, 1430-4.

Kuo, C. S., Hu, H. T., Lin, R. M., Huang, K. Y., Lin, P. C., Zhong, Z. C. & Hseih, M. L. 2010. Biomechanical analysis of the lumbar spine on facet joint force and intradiscal pressure--a finite element study. *BMC Musculoskelet Disord,* 11, 151.

Kurtz, S. M. & Edidin, A. 2006. Spine Technology Handbook.

Kurutz, M. & Oroszvary, L. 2010. Finite element analysis of weightbath hydrotraction treatment of degenerated lumbar spine segments in elastic phase. *J Biomech,* 43, 433-41.

Kurutz, M. & Oroszváry, L. 2010. Finite element analysis of weightbath hydrotraction treatment of degenerated lumbar spine segments in elastic phase. *Journal of Biomechanics*.

Leboeuf-Yde, C. 2000. Body Weight and Low Back Pain. *Spine,* 25.

Lee, M., Kelly, D. W. & Steven, G. P. 1995. A model of spine, ribcage and pelvic responses to a specific lumbar manipulative force in relaxed subjects. *Journal of Biomechanics*.

Lucas, D. B., Bresler, B. & Florence Hellman Ehrman Endowment Fund for Orthopedic, R. 1961. *Stability of the ligamentous spine*, San Francisco, Biomechanics Laboratory, University of California.

Manchikanti, L., Hirsch, J. A., Falco, F. J. & Boswell, M. V. 2016. Management of lumbar zygapophysial (facet) joint pain. *World J Orthop,* 7**,** 315-37.

Manusov, E. G. 2012. Evaluation and diagnosis of low back pain. *Prim Care,* 39**,** 471-9.

Markolf, K. L. & Morris, J. M. 1974. The structural components of the intervertebral disc. A study of their contributions to the ability of the disc to withstand compressive forces. *The Journal of bone and joint surgery. American volume*.

Miller, M. D. & Thompson, S. R. 2003. DeLee, Drez and Miller's orthopaedic sports medicine : principles and practice. *Philadelphia, PA: Saunders*.

Muscolino, J. E. 2014. *Manual Therapy for the Low Back and Pelvis: A Clinical Orthopedic Approach*.

Netter, F. H. 2014. Atlas of Human Anatomy. *Elsevier Health Sciences*.

Niddk 2001. Understanding Adult Obesity. *Weight-control Information Network*.

Nordin, M. & Frankel, V. H. 2001. *Basic Biomechanics of the Musculoskeletal System*, Lippincott Williams & Wilkins.

Olivier Y. Rolin, W. E. C. I. Biomechanics of the Spine.

Panjabi, M. M. 2003. Clinical spinal instability and low back pain. *Journal of Electromyography and Kinesiology*.

Panjabi, M. M., Oxland, T. R., Yamamoto, I. & Crisco, J. J. 1994. Mechanical behavior of the human lumbar and lumbosacral spine as shown by three-dimensional load-displacement curves. *The Journal of Bone & Joint Surgery*, 76**,** 413-424.

Park, W. M., Kim, K. & Kim, Y. H. 2013. Effects of degenerated intervertebral discs on intersegmental rotations, intradiscal pressures, and facet joint forces of the whole lumbar spine. *Comput Biol Med*, 43**,** 1234-40.

Patwardhan, A. G., Havey, R. M., Meade, K. P., Lee, B. & Dunlap, B. 1999. A follower load increases the load-carrying capacity of the lumbar spine in compression. *Spine*.

Peng, T., Perez, A. & Pettee Gabriel, K. 2018. The Association Among Overweight, Obesity, and Low Back Pain in U.S. Adults: A Cross-Sectional Study of the 2015 National Health Interview Survey. *J Manipulative Physiol Ther*, 41**,** 294-303.

Pintar, F. A., Yoganandan, N., Myers, T., Elhagediab, A. & Sances, A. 1992. Biomechanical properties of human lumbar spine ligaments. *Journal of Biomechanics*.

Raj, P. P. 2008. Intervertebral disc: anatomy-physiology-pathophysiology-treatment. *Pain Pract,* 8**,** 18-44.

Ranu, H. S. 1990. Measurement of pressures in the nucleus and within the annulus of the human spinal disc: Due to extreme loading. *Proceedings of the Institution of Mechanical Engineers, Part H: Journal of Engineering in Medicine*.

Renner, S. M., Natarajan, R. N., Patwardhan, A. G., Havey, R. M., Voronov, L. I., Guo, B. Y., Andersson, G. B. J. & An, H. S. 2007. Novel model to analyze the effect of a large compressive follower pre-load on range of motions in a lumbar spine. *Journal of Biomechanics*.

Rohlmann, A., Burra, N. K., Zander, T. & Bergmann, G. 2007. Comparison of the effects of bilateral posterior dynamic and rigid fixation devices on the loads in the lumbar spine: a finite element analysis. *Eur Spine J,* 16**,** 1223-31.

Rohlmann, A., Neller, S., Claes, L., Bergmann, G. & Wilke, H. J. 2001. Influence of a follower load on intradiscal pressure and intersegmental rotation of the lumbar spine. *Spine*.

Rohlmann, A., Zander, T., Schmidt, H., Wilke, H. J. & Bergmann, G. 2006. Analysis of the influence of disc degeneration on the mechanical behaviour of a lumbar motion segment using the finite element method. *J Biomech,* 39**,** 2484-90.

Samandouras, G. 2010. *The Neurosurgeon's Handbook*, OUP Oxford.

Sarathi Banerjee, P. 2013. Morphological and Kinematic Aspects of Human Spine – As Design Inputs for Developing Spinal Implants. *Journal of Spine,* 02.

Schmidt, H., Heuer, F., Claes, L. & Wilke, H. J. 2008. The relation between the instantaneous center of rotation and facet joint forces - A finite element analysis. *Clin Biomech (Bristol, Avon),* 23**,** 270-8.

Schmidt, H., Heuer, F., Drumm, J., Klezl, Z., Claes, L. & Wilke, H. J. 2007. Application of a calibration method provides more realistic results for a finite element model of a lumbar spinal segment. *Clin Biomech (Bristol, Avon),* 22**,** 377-84.

Schmidt, H., Heuer, F., Simon, U., Kettler, A., Rohlmann, A., Claes, L. & Wilke, H. J. 2006. Application of a new calibration method for a three-dimensional finite element model of a human lumbar annulus fibrosus. *Clin Biomech (Bristol, Avon),* 21**,** 337-44.

Schulte, T. L., Hurschler, C., Haversath, M., Liljenqvist, U., Bullmann, V., Filler, T. J., Osada, N., Fallenberg, E. M. & Hackenberg, L. 2008. The effect of dynamic, semi-rigid implants on the range of motion of lumbar motion segments after decompression. *Eur Spine J,* 17**,** 1057-65.

Schwarzer, A. C., Aprill, C. N., Derby, R., Fortin, J., Kine, G. & Bogduk, N. 1994. The Relative Contributions of the Disc and Zygapophyseal Joint in Chronic Low Back Pain. *Spine*, 19**,** 801-806.

Shiri, R., Karppinen, J., Leino-Arjas, P., Solovieva, S. & Viikari-Juntura, E. 2010. The association between obesity and low back pain: a meta-analysis. *Am J Epidemiol*, 171**,** 135-54.

Shiri, R., Solovieva, S., Husgafvel-Pursiainen, K., Taimela, S., Saarikoski, L. A., Huupponen, R., Viikari, J., Raitakari, O. T. & Viikari-Juntura, E. 2008. The association between obesity and the prevalence of low back pain in young adults: the Cardiovascular Risk in Young Finns Study. *Am J Epidemiol*, 167**,** 1110-9.

Smith, K. B. & Smith, M. S. 2016. Obesity Statistics. *Prim Care*, 43**,** 121-35, ix.

Teo, E. C., Lee, K. K., Qiu, T. X., Ng, H. W. & Yang, K. 2004. The biomechanics of lumbar graded facetectomy under anterior-shear load. *IEEE Trans Biomed Eng*, 51**,** 443-9.

Urban, J. P. & Roberts, S. 2003. Degeneration of the intervertebral disc. *Arthritis Res Ther*, 5**,** 120.

Vincent, H. K., Heywood, K., Connelly, J. & Hurley, R. W. 2012. Obesity and weight loss in the treatment and prevention of osteoarthritis. *PM R*, 4**,** S59-67.

Vismara, L., Menegoni, F., Zaina, F., Galli, M., Negrini, S. & Capodaglio, P. 2010. Effect of obesity and low back pain on spinal mobility: a cross sectional study in women. *J Neuroeng Rehabil,* 7**,** 3.

Walker, B. F. 2000. The Prevalence of Low Back Pain: A Systematic Review of the Literature from 1966 to 1998. *Journal of Spinal Disorders,* 13**,** 205-217.

Wang, L., Zhang, B., Chen, S., Lu, X., Li, Z. Y. & Guo, Q. 2016. A Validated Finite Element Analysis of Facet Joint Stress in Degenerative Lumbar Scoliosis. *World Neurosurgery*.

Weishaupt, D., Zanetti, M., Hodler, J. & Boos, N. 1998. MR imaging of the lumbar spine: prevalence of intervertebral disk extrusion and sequestration, nerve root compression, end plate abnormalities, and osteoarthritis of the facet joints in asymptomatic volunteers. *Radiology,* 209**,** 661-6.

White, A. A. & Panjabi, M. M. 1990. *Clinical biomechanics of the spine,* Lippincott.

Zahari, S. N., Abd Latif, M. J. & Kadir, M. R. A. 2014. The influence of preload application for vertebra segment in finite element modelling. *IECBES 2014, Conference Proceedings - 2014 IEEE Conference on Biomedical Engineering and Sciences: "Miri, Where Engineering in Medicine and Biology and Humanity Meet"*.

Zahari, S. N., Latif, M. J. A., Rahim, N. R. A., Kadir, M. R. A. & Kamarul, T. 2017. The Effects of Physiological Biomechanical Loading on Intradiscal Pressure and Annulus Stress in Lumbar Spine: A Finite Element Analysis. *J Healthc Eng,* 2017**,** 9618940.

Zander, T., Rohlmann, A. & Bergmann, G. 2004. Influence of ligament stiffness on the mechanical behavior of a functional spinal unit. *J Biomech*, 37**,** 1107-11.

Zhang, Z., Fogel, G. R., Liao, Z., Sun, Y. & Liu, W. 2018. Biomechanical analysis of lumbar interbody fusion cages with various lordotic angles: a finite element study. *Comput Methods Biomech Biomed Engin*, 21**,** 247-254.

APPENDIX A1

L1 anterior vertebrae dimension details

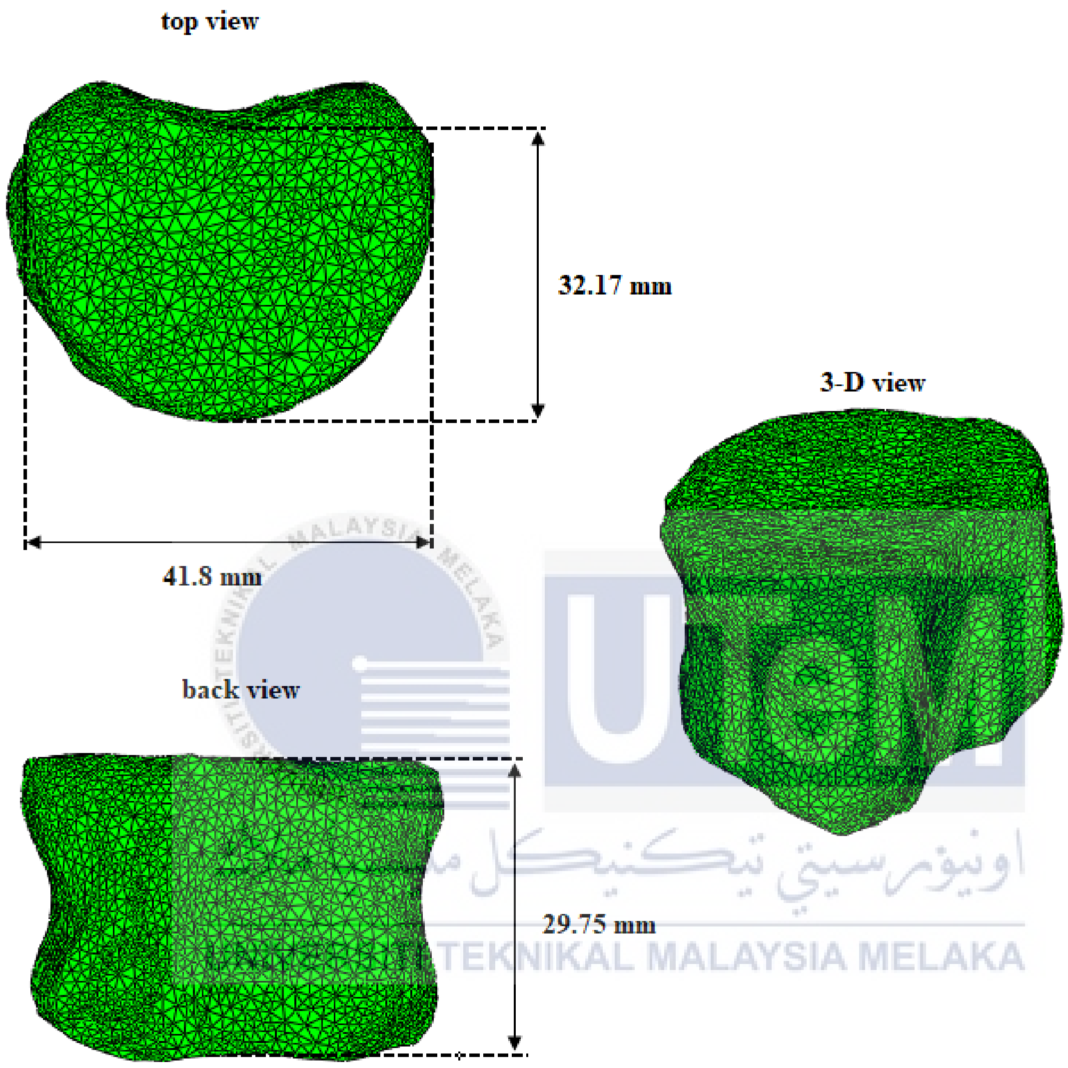

APPENDIX A2

Disc Specification (Length and Width)

		Length (mm)	Width (mm)
Nucleus	Nucleus location	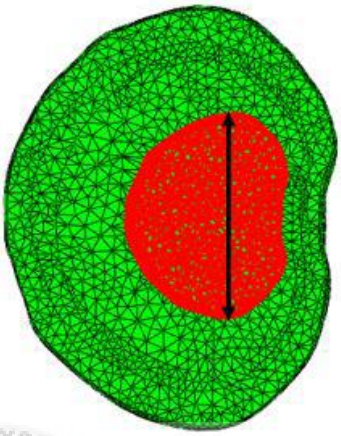	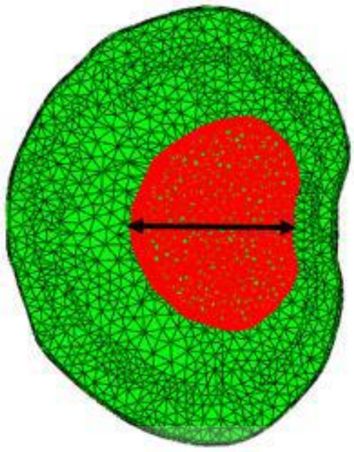
	L1/L2	20.20	16.16
	L2/L3	20.82	16.66
	L3/L4	21.35	16.73
	L4/L5	21.42	16.76
Disc	Disc location	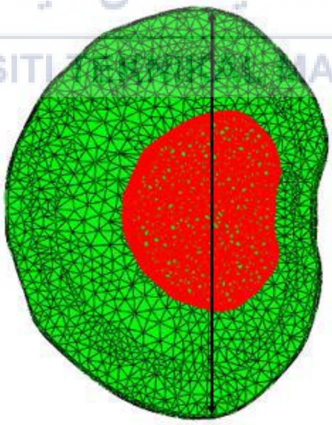	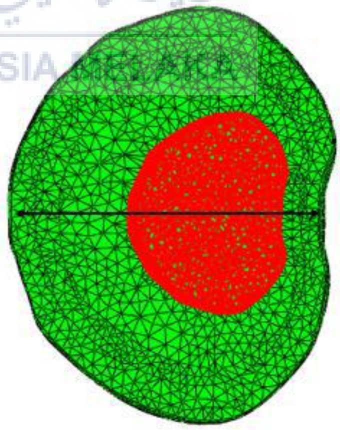
	L1/L2	44.49	34.96
	L2/L3	45.04	33.48
	L3/L4	47.27	33.10
	L4/L5	51.83	48.99

APPENDIX A3

Disc Specification (Thickness)

		Anterior	Posterior
Nucleus	**Nucleus location**	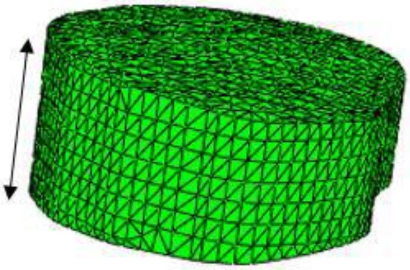	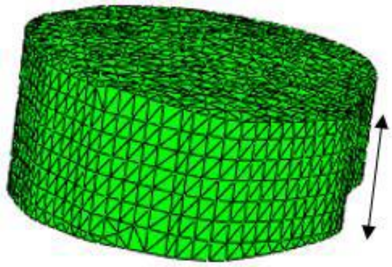
	L1/L2	8.31	5.67
	L2/L3	9.47	7.51
	L3/L4	10.17	8.18
	L4/L5	10.20	6.8
Disc	**Disc location**	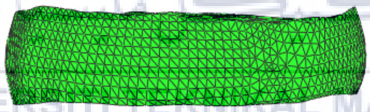	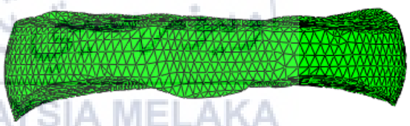
	L1/L2	9.39	7.77
	L2/L3	10.25	8.05
	L3/L4	11.43	10.04
	L4/L5	13.42	6.83

APPENDIX A4

Superior and Inferior Facet Joint Specification

		Anterior	**Posterior**
Superior	**Facet location**	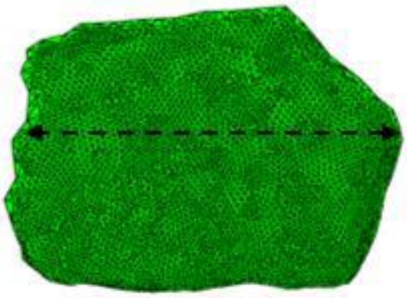	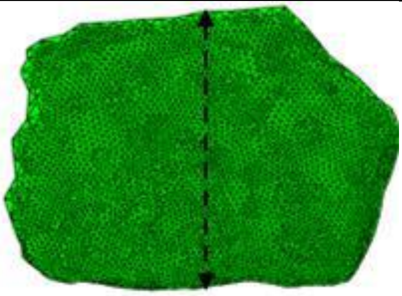
	L2	15.25	12.23
	L3	16.59	12.82
	L4	16.71	16.09
	L5	18.63	16.86
Inferior	**Facet location**		
	L2	13.92	10.73
	L3	14.29	12.22
	L4	17.44	13.19
	L5	18.57	11.86

APPENDIX B1

Case study – simulation data results

						Contact Pressure						
		inferior						superior				
Flexion		Left			Right			Left			Right	
Load	Normal	Overweight	Obese	Normal	Overweight	Obese	Normal	Overweight	Obese	Normal	Overweight	Obese
L1-L2	0	0	0	0	0	1.781	0	0	0	0	0	1.841
L2-L3	0	1.236	1.536	0	0	0	0	0.856	1.137	0	0	0
L3-L4	0	0	3.17	0	0	0	0	0	1.913	0	0	0
L4-L5	0	0	0	0	0	0	0	0	0	0	0	0
		inferior						superior				
Extension		Left			Rght			Left			Right	
Load	Normal	Overweight	Obese	Normal	Overweight	Obese	Normal	Overweight	Obese	Normal	Overweight	Obese
L1-L2	8.456	8.785	10.33	6.794	7.085	7.813	9.341	9.055	10.52	6.781	7.028	7.393
L2-L3	0	0	0	6.375	6.553	7.179	0	0	0	6.265	6.472	7.238
L3-L4	8.746	9.129	9.775	8.999	9.563	10.73	7.839	8.203	9.074	8.201	8.479	9.148
L4-L5	0	0	4.562	4.603	4.737	5.432	0	0	4.83	4.859	5.209	5.468

					Stress at	Capsular	Ligament			
		Left					Right			
	L1-L2	L2-L3	L3-L4	L4-L5		L1-L2	L2-L3	L3-L4	L4-L5	
Normal	17.13929	8.02318	16.69718	6.377925		20.14737	12.89076	13.58821	10.76657	
Overweig	18.07909	8.081304	17.61224	5.737866		21.1107	13.17674	14.51136	10.65776	
Obese	20.01294	8.216625	19.48654	10.63562		22.98209	13.51232	16.55075	12.15716	

		ROM (degree)		
		Normal	Overweight	Obese
Flexion	L1-L2	3.29	2.96	2.27
	L2-L3	4.88	4.53	3.63
	L3-L4	5.55	5.29	4.4
	L4-L5	4.69	4.52	3.81
Extension	L1-L2	4.37	4.44	4.56
	L2-L3	5.2	5.28	5.48
	L3-L4	4.26	4.3	4.42
	L4-L5	3.34	3.44	3.74